

Sudan University of Science and Technology
Collage of Graduate Studies



**shear capacity of R.C Deep beams strengthened by Carbon
Fiber Polymer (CFP) by using Different Methods**

سعة القص للعارضات العميقة المسلحة المقواة بالالياف الكربونية باستخدام طرق
مختلفة

**A Thesis Submitted in Partial Fulfillment for the Requirements of
MSc Degree in Civil Engineering (Structural Engineering)**

Prepared By:

Abdallah Gassem Elseed Mohamed Ahmed

Supervised By:

Dr.Abusamra Awad Attaelmanan

March 2016

بِسْمِ اللّٰهِ

الرّحْمٰنِ

الرّحِیْمِ

الآيه القرآنيه

“وَلَقَدْ آتَيْنَا لَقْمَانَ الْحِكْمَةَ أَنْ شَكَرَ لِلَّهِ وَمَنْ
يَشْكُرْ فَإِنَّمَا يَشْكُرُ لِنَفْسِهِ وَمَنْ كَفَرَ فَإِنَّ اللَّهَ غَنِيٌّ

حَمِيدٌ”

لقمان (12)



Dedication

To my mother, wife and brother who have continuously encouraged and patiently.

.

Acknowledgements

I would like to thank my supervisor Dr. Abusamra Awad Attaelmanan for his guidance and patience during all stages of this research.

ABSTRACT

In this study the carbon Fiber Reinforcement Polymer (CFRP) on increasing shear capacity of reinforcement concrete deep beams. Different methods of strengthening of structures were used to calculate shear capacity. These methods were ACI, Triantafillou, Carolin and Zhichao.

The parameters used in this work were thickness of (CFRP), depth of beam and concrete compressive strength using three configuration of (CFRP) such as fully wrapped, U and two sides wrapped. The design of shear strength were prepared by Microsoft Excel spread sheets for the three configuration of wrapping to study the effect of different parameters on shear capacity of deep beams. It was found for the fully wrapped, ACI method appears to predict the (CFRP) shear contribution with a relatively high discrepancy with respect to Triantafillou, Carolin and Zhichao and Triantafillou method overestimates results of shear capacity for U, or two sides wrapped with respect to ACI Method

التجريد

تم إستخدام ألياف الكربون لزيادة سعة العارضات العميقة للقص من خلال عدة طرق مختلفة للتقوية تم وضعها بواسطة (ACI, Triantafillou, Carolin and Zhichao) .

والمغيرات المستخدمة في هذا العمل هي سماكة الياف الكاربون وعمق المقطع الخرساني ومقاومة الخرسانة وذلك بإستخدام ثلاثة أشكال مختلفة للتقوية (تغليف كامل للمقطع, وتغليف علي شكل U وأخيراً تغليف بإتجاهين فقط).

تم التصميم بواسطة برنامج Microsoft Excel بإستخدام الأشكال الثلاثة السابقة وبتطبيق الطرق الاربعة المذكورة ,حيث اسفرت النتائج بأن طريقة ACI تعطي أعلي نتائج في حالة التغليف الكامل للمقطع مقارنة مع الطرق الثلاثة الأخرى, اما في حالة التغليف علي شكل U والتغليف بإتجاهين فقط فكانت طريقة (Triantafillou) تعطي مساهمة لزيادة سعة القص للعارضات اكبر من طريقة (ACI).

LIST OF CONTENTS

Contents		Pages
	الإيه	I
	Dedication	II
	Acknowledgements	III
	Abstract: English	IV
	Abstract: Arabic	V
	List of Contents	VI
	List of Tables	IX
	List of Figures	X
	List of Abbreviations	XII
Chapter One	INTRODUCTION	
1.1	Introduction	1
1.2	Research Objectives	3
1.3	Research Methodology	3
1.4	Research Organization	4
Chapter Two	LITERATURE REVIEW	
2.1	Introduction	6
2.2	Factors affecting behavior of deep beams	6
2.3	Types of shear reinforcement	8
2.3.1	Reinforcement details	8
2.3.1	Method of load application	10
2.4	Comparison between deep beams and ordinary beams	10
2.5	Failure mode of deep beams	11
2.5.1	Diagonal compression failure	11
2.5.2	The second type of shear failure is a diagonal tension failure	11
2.6	The importance of RC deep beams	13

2.7	The Need for Strengthening	14
2.8	The Importance of FRP Polymers	15
2.8.1	FRP Configuration	16
2.8.2	FRP Orientations	16
2.9	Failure mechanism of reinforced concrete beams	17
2.9.1	Diagonal tension failure	17
2.9.2	Shear compression failure	19
2.10	Previous experimental work	19
2.11	Previous analytical work on deep beams	28
2.12	Traditional methods and Codes of Practices for Calculating RC Beams Capacity	30
Chapter three	MATERIALS PROPERTIES AND SUMMARY OF DESIGN EQUATIONS FROM VARIOUS GUIDELINES	
3.1	Introduction	34
3.2	Comparison of different method with Design Guidelines	34
3.2.1	ACI equation	34
3.2.2	Triantafillou and Anton 2000 equation for FRP contribution	39
3.2.3	Carolin and Taljsten 2005 equation	41
3.2.4	Zhichao and Cheng 2005 equation	44
3.3	Material properties and codes of practice used in this study	47
Chapter Four	RESULTS AND DISCUSSION	
4.1	Introduction	41
4.2	Effect of FRP Thickness on Shear Strength of RC	49

	Deep beams	
4.3	Effect of Concrete Strength on Beams capacity	52
4.4	Effect of beam depth (d) on concrete shear strength (V_c)	55
4.5	Discussion of results	58
Chapter Five	CONCLUSIONS AND RECOMMENDATIONS	
5.1	Conclusions	60
5.2	Recommendations	60
	References	61
	Appendix 1 ACI code calculation sheet	66
	Appendix 2 (Traintafillou and Anton 2000)	81
	Appendix 3 carolin and taljsten 2005	89
	Appendix 4 Zhichao and cheng 2005	94

LIST OF TABLES

Table	Title	Page
3.1	The materials properties of Deep beam	
4.1	The influence of FRP thickness on shear capacity (kN) using different method	
4.2	The influence of concrete strength on concrete shear strength	
4.3	The influence of Beam Depth on shear Strength	

LIST OF FIGURES

Figure	Title	Page
2.1	Web steel and main longitudinal steel	
2.2.a	Beam without web reinforcement.	
2.2.b	Beam with horizontal reinforcement.	
2.2.c	Beam with vertical web reinforcement	
2.3	Cracks in beam due to excessive load	
2.4	Various composite materials	
2.5	Shear strengthening configurations using FRP	
2.6	Degree of FRP coverage and fiber orientation	
2.7	Crack patterns and shear failure	
2.8	shear strength v_s . provided by shear reinforcement	
3.1	Illustration of the dimensional variables used in shear-strengthening calculations for repair, retrofit, or strengthening using CFRP laminates.	
3.2	Flow Chart of ACI method	
3.3	Flow chart Triantafillou and Anton method 2000	
3.4	Illustration of the (β, ϕ, α)	
3.5	flow chart fo carolin and Taljsten 2005 method	
3.6	flow chart of Zhichao and Cheng 2005 equation	
3.7	Geometrical details of proposed RC beams	
4.1.a	Effect of FRP thickness on concrete shear strength for different guidelines, full wrap	
4.1.b	Effect of FRP thickness on concrete shear strength for different guidelines, U wrap	
4.1.c	Effect of FRP thickness on concrete shear strength for different guidelines , two sides	
4.2. a	Effect of concrete strength on concrete shear strength	

- for different guidelines , full wrap
- 4.2. b Effect of concrete strength on concrete shear strength
for different guidelines , U- wrap
 - 4.2. c Effect of concrete strength on concrete shear strength
for different guidelines , two sides
 - 4.3.a Effect of beam depth on concrete shear strength (V_c) for
different guidelines , full wrap
 - 4.3.b Effect of beam depth on concrete shear strength (V_c) for
different guidelines U wrap
 - 4.3.c Effect of beam depth on concrete shear strength (V_c) for
different guidelines two sides

List of Abbreviations

A _f	area of FRP external reinforcement, (mm ²)
A _{f_v}	area of FRP shear reinforcement with spacing s
b _w	web width or diameter of circular section,
d	distance from extreme compression fiber to centroid of tension reinforcement, (mm)
d _f	effective depth of FRP flexural reinforcement
E _c	modulus of elasticity of concrete, (MPa)
E _f	tensile modulus of elasticity of FRP, (MPa)
E _s	modulus of elasticity of steel, (MPa)
f _c '	specified compressive strength of concrete, (MPa)
f _{tu}	design ultimate tensile strength of FRP, (MPa)
F _y	specified yield strength of nonprestressed steel reinforcement, (MPa)
H	overall thickness or height of a member, (mm)
k	ratio of depth of neutral axis to reinforcement depth measured from extreme compression fiber
k ₁	modification factor applied to κ _v to account for concrete strength
k ₂	modification factor applied to κ _v to account for wrapping scheme
k _f	stiffness per unit width per ply of the FRP reinforcement, (N/mm);
L _e	active bond length of FRP laminate, (mm)
t _f	nominal thickness of one ply of FRP reinforcement, (mm)
V _c	nominal shear strength provided by concrete with steel flexural reinforcement, (N)
V _f	nominal shear strength provided by FRP stirrups, (N)

V_n	nominal shear strength, (N)
V_s	nominal shear strength provided by steel stirrups, (N)
w_f	width of FRP reinforcing plies, (mm)
ϵ_f	strain level in the FRP reinforcement, (mm/mm)
ϵ_{fe}	effective strain level in FRP reinforcement attained at failure, (mm/mm)
ϵ_{fu}	design rupture strain of FRP reinforcement, (mm/mm)
ψ_f	FRP strength reduction factor
ψ_f	0.85 for flexure (calibrated based on design material properties)
ψ_f	0.85 for shear (based on reliability analysis) for three-sided FRP U-wrap or two-sided strengthening schemes
ψ_f	0.95 for shear fully wrapped sections
ϕ	strength reduction factor
κ_v	bond-dependent coefficient for shear
ρ_f	FRP reinforcement ratio

CHAPTER ONE

INTRODUCTION

CHAPTER ONE

INTRODUCTION

1.1 Introduction

Deep beams are structural elements loaded as beams in which a significant amount of the load is transferred to the supports by compression thrust joining the load and the reaction. As result, the strain distribution is no longer considered linear and the shear deformations become significant when compared to pure flexure. Reinforced concrete (R.C) deep beams, which fail with shear compression, are the structural members having a shear span to effective depth ratio, a_v/d , not exceeding 1.0. The ACI code defines a deep beam as a structural member whose span-depth ratio (L/H) is 5 or less.

Some investigators have decided that the shear span-effective depth ratio a_v/d is more meaningful to define deep beam, and that a beam could be considered deep if shear span to effective depth ratio (a_v/d) < 0.5.

R.C deep beams have many useful applications in buildings structures such as transfer girders, wall footings, foundation pile caps, floor diaphragms and shear walls. Beams of this type often arise in the construction of bins, hoppers, or similar structures, as well as pile caps and transfer girders.

Particularly, the use of deep beams at the lower levels in tall buildings for both residential and commercial purposes has increased rapidly because of their convenience and economic efficiency. Generally, deep beams are regarded as members loaded on their top extreme fibers in compression and supported on the opposite side. In all these cases design based on ordinary straight-line distribution of bending stresses adopted in a shallow beams is not valid, since the simple theory of flexure takes no account of

the effect of normal pressures on the top and bottom edges of the beam caused by the loads and reactions.

The effect of these normal pressures on the stress distribution in deep beams is such that the distribution of bending stresses on vertical sections is not linear and the distribution of the shear stress is not parabolic. Consequently, a transverse section which is plane before bending does not remain approximately plane after bending and the neutral axis does not usually lie at the mid depth, its position being variable in a span wise direction.

Strengthening with externally bonded CFRP laminates has been shown to be applicable to many kinds of structures. This method has been applied to strengthen such structures as columns, beams, walls, slabs, and so on. The use of external CFRP reinforcement may be classified as flexural strengthening improving the ductility of compression members, and shear strengthening.

Shear failure is catastrophic and occurs usually without advance warning; thus, it is desirable that the beam fail in flexure rather than in shear. Many existing RC members are found to be deficient in shear strength and need to be repaired. Deficiencies occur for several reasons, including insufficient shear reinforcement or reduction in steel area because of corrosion, increased service load, as CFRP provides an excellent solution in these situations.

The use of Fiber Reinforced Polymer (CFRP) is becoming a widely accepted solution for repairing and strengthening ageing in the field of civil engineering around the world, fiber-reinforced polymer (CFRP) use for the rehabilitation of beams and slabs started about 15 years ago with the pioneering research performed at the Swiss Federal Laboratories for Materials Testing and Research. (CFRP) composites, used in the repair of

beams and slabs as external tensile reinforcement, increase the strength (ultimate limit state) and the stiffness (serviceability limit state) of the structure. Repair with (CFRP) is thus motivated by requirements for earthquake strengthening, higher service loads, smaller deflections, or simply to substitute for deteriorated steel reinforcement

1.2 .Research Objectives

The Objectives of research are:

1. To Study shears capacity and behavior of RC deep beams with different Configurations of fiber reinforcement polymer (CFRP) strengthening type.
2. To study the effect of FRP thickness in strengthening of RC deep beams.
3. To study the effect of concrete depth on shear capacity of deep beams.
4. To use ACI code for conducting the real behavior of shear capacity in RC deep beams strengthened by (CFRP) and compare results with other guidelines work so as to verify them.
5. To investigate the concrete strength effects on the behavior of concrete beams.

1.3. Research Methodology

The methodology adopted to achieve the above mentioned objectives of this study are:

1- Literature Review: basic concepts will be revised and related literature and relevant data will be collected. Then, the main features of the proposed work will be pointed out.

2- Theoretical concept: rectangular concrete beams deep beams will be studied and analyzed under shear loads with different parameters.

A parametric study was conducted to clarify their influence on shear capacity. Based on this study, a prediction model was proposed by considering all common parameters that influence the ultimate shear capacity of a strengthened beam including concrete strength , effective height of the beam , CFRP thickness , and strengthening configuration (completely wrapped, U-jacketing, and side bonding).

3- Analysis of the Results: the results arising from the second stage above are tabulated and analyzed.

1.4. Research Organization

The present thesis is divided into five chapters.

The general introduction to retrofit the reinforced concrete (RC) beams and its importance in different engineering fields along with the objective of the present work are outlined in chapter 1.

A review comprising of literature on strengthening of different types of beams under different load conditions are presented in chapter 2. The critical observations on earlier published works are highlighted and the scope of the present research work is outlined.

Chapter 3 deals with the description of the theoretical guidelines which used in this study. The constituent materials, the beam specimen, and analysis methods using different guidelines equation are presented.

Chapter 4 deals with the analysis and discussion of the results, which conducted from previous guidelines for computing the shear capacity of the strengthened beams.

The important conclusions and the scope for further extension of the present work are outlined in chapter 5.

A list of important references cited in the present thesis is presented at the end.

CHAPTER TWO

LITERATURE REVIEW

CHAPTER TWO

LITERATURE REVIEW

2.1. Introduction

Early analysis of reinforced concrete deep beams was based on the classical theory of elasticity with the beam assumed as homogenous. Reinforcement was placed in regions where tensile stresses exceed the estimated strength of the concrete. Some of the earliest work in this area was performed by Dischinger ^{1} and distributed as a design aid by the Portland Cement Association.

The use of carbon-fiber-reinforcement polymer(CFRP) in strengthening reinforced concrete(RC) structures has become an increasing popular retrofit technique. The technique of strengthening RC structures by using externally bonded CFRP laminates started in the 1980 and has since attracted researchers (Berset 1992; Chajes et al,1995; Khalifa et al,1996; Triantafillou 1998; Uji 1992; Zhang and Hsu 2000,2002) from around the world .

2.2. Factors affecting behavior of deep beams

As the a_v/d ratio of deep beam decreases from about 2.5 to 0.0, shear reinforcement perpendicular to the longitudinal axis becomes less effective than that in ordinary beam. At the same time, distributed reinforcement parallel to the longitudinal axis will increase shear capacity of shear-friction. Diagonal reinforcement is also effective in resisting shear.

Many tests have established that the failure mode is strongly dependent on the shear-span/depth ratio a_v/d :

* $a_v/d > 6$: beams with such a high a_v/d ratio usually fail in bending.

* $6 > a_v/d > 2.5$: beams with a_v/d lower than about 6 tend to fail in shear.

If the a_v/d ratio is relatively high, the diagonal crack would rapidly spread to e , resulting in collapse by splitting the beam into two pieces. This mode of failure is called diagonal-tension failure.

* $2.5 > a_v/d > 1$: for a_v lower than about 2.5 but greater than 1.0, the diagonal crack often forms independently and not as development of a flexural crack. The beam usually remains stable after such cracking.

Further increase in the force V will cause the diagonal crack to penetrate into the concrete compression zone at the loading point, until eventually crushing failure of the concrete occurs there, sometimes explosively (shaded portion). This failure mode is called shear-compression failure; for this mode, the ultimate load is sometimes more than twice that at diagonal cracking.

* $a_v/d < 1.0$: the behavior of beams with such low a_v/d ratio approaches that of deep beams. The diagonal crack forms approximately along a line joining the loading and support points. When the crack has penetrated sufficiently deeply into the concrete zone at the loading point, or, more frequently, at the support point, crushing failure of the concrete occurs. For a deep beam failure mode, the ultimate load is often several times that at diagonal cracking.

The shear strength is affected by several factors such as:

1- Concrete strength

The dowel action capacity, the aggregate interlock capacity and the compression-zone capacity generally all increase with the concrete strength.

2- Tension steel ratio

The tension steel ratio affects shear strength mainly because a low A_s/bd value reduces the dowel shear capacity and also leads to wider crack widths, which in turn reduce the aggregate-interlock capacity.

3- Strength of longitudinal reinforcement

Provided the steel ratio is kept constant, the characteristic strength of the longitudinal reinforcement has little effect on shear strength.

4- Aggregate type

The type of aggregate affects shear strength mainly through its effect on aggregate interlock capacity.

5- Beam size

The ultimate shear stress reduces with the beam size particularly the beam depth; that is, larger beams are proportionately weaker than smaller beams. This is probably because in practice the aggregate interlock capacity does not increase in the same proportion as the beam size.

6-Shear-span/depth ratio (M/Vd)

The ultimate shear stress at a beam section increase rapidly as the M/Vd ratio is reduced below about 2, where M is the bending moment, V the shear force and d the effective depth; this is true for either distributed loading or concentrated loading. For two-point loading, the critical M/Vd ratio occurs at the loading point, where:

$$\mathbf{M/Vd = a_v /d}$$

2. 3. Types of shear reinforcement

As the a_v/d ratio of deep beam decreases from about 2.5 to 0.0, shear reinforcement perpendicular to the longitudinal axis becomes less effective than that in ordinary beam. At the same time, distributed reinforcement parallel to the longitudinal axis will increase shear capacity of shear-friction. Diagonal reinforcement is also effective in resisting shear ^{2}.

2.3.1. Reinforcement details

The development of inclined cracking tends to cause an increase in the stress in flexural tension reinforcement at the base of the crack. In deep beams, inclined cracking may extend the full length of the shear span. If

the shear reinforcement is not fully effective **Fig.2.1**, high tensile stresses will develop in the longitudinal reinforcement at sections where the resultant moment is zero **Fig.2.2** (a,b,c). Sufficient anchorage length of main reinforcement must be provided to resist this tension.

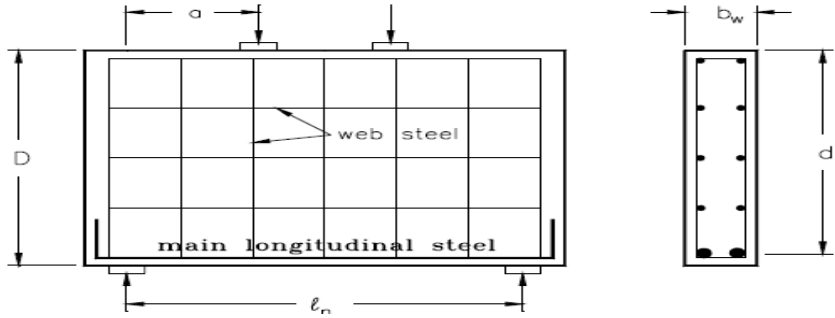
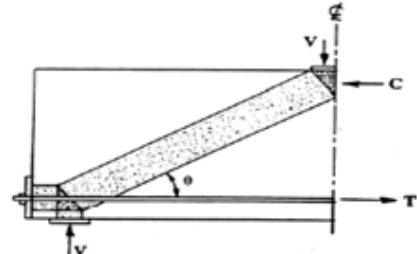
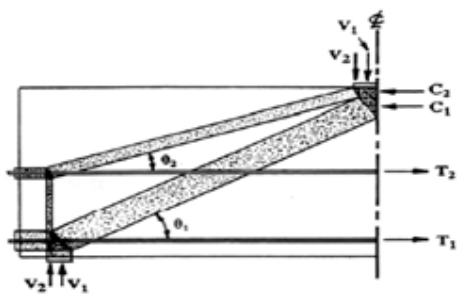


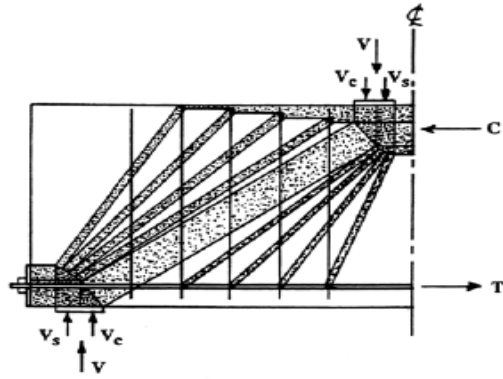
Fig.2.1 Web steel & main longitudinal steel



(a) Beam without web reinforcement.



(b) Beam with horizontal reinforcement.



(c) Beam with vertical web reinforcement

Fig. 2.2. Beam Reinforcement.

2.3.2. Method of load application

Load may be applied to beams on the extreme compression or tension fibers. The main effect of applying loads on the compression face to a deep beam without web reinforcement is to increase the ultimate shear capacity above the shear causing inclined cracking.

2.4. Comparison between deep beams and ordinary beams

1- Deep beams

- Plane section before bending does not remain plane after bending.
- The resulting strain is nonlinear.
- Shear deformations become significant compared to pure flexure.
- The stress block is nonlinear even at the elastic stage.
- It is subjected to two-dimensional state of stress.

2- Ordinary beams

- Plane section before bending remains plane after bending.
- The strain is linear
- Shear deformation is neglected.
- The stress block is considered linear at the elastic stage.
- It is subjected to one-dimensional state of stress.

2.5. Failure mode of deep beams

The failure of deep beams subjected to either central point load or two symmetrical point loads is related to the failure of the tied arch which is formed in the beam after diagonal cracking. According to de ^{3}, the primary modes of failure of the tied arch are flexure failure and shear failure. A flexural failure occurs either when the concrete rib of the tied-arch fails by crushing at the crown or the tension tie ruptures. The failure is termed flexure failure because the full flexural capacity and ductility are realized. A shear failure contains two types:

2.5.1 Diagonal compression failure

In this type of failure an inclined crack first develops nearly along a line joining the load point and the support point. After further increase in load, a second inclined crack parallel to the previous crack appears. The final failure is due to the destruction of the portion of concrete between these two cracks which acts as a strut between the load and support point.

2.5.2 The second type of shear failure is a diagonal tension failure

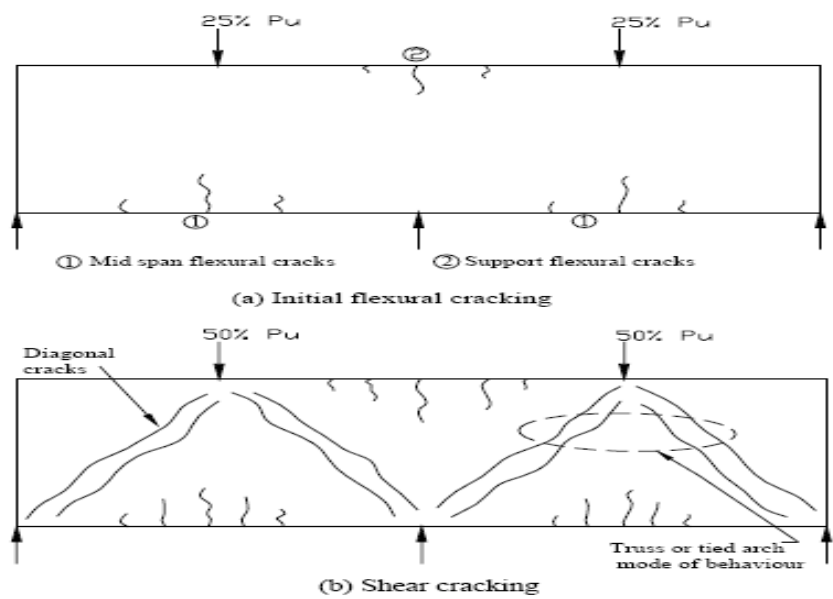
In this mode failure occurs by a clean and sudden fracture nearly along a line joining either support with the nearest loading point. The failure is similar to splitting of a cylinder under diagonal compression. This mode sometimes called shear-proper failure.

Bresler and Macgregor have included anchorage failure and bearing failure as deep beam failure modes along with the flexure and shear failure mentioned above. These two additional modes of failure are generally undesirable and are not limited to deep beams although the geometry and behavior of deep beams have increased the likelihood of their occurrence. Anchorage failure results from the very high tension stresses in the main longitudinal reinforcement in the region near the

supports. Special anchorage provisions, such as hooking the bars, can be used to prevent this mode of failure. Baring failures on the other hand result from the high vertical stresses at the support and load points. Adequate design and detailing of the bearing and load blocks will prevent this mode of failure. ^{4}

In summary, a prediction of deep beam failure load is usually limited to a prediction of either flexure or shear failure modes, as anchorage and bearing failure are undesirable failure modes which can be eliminated by proper design and detailing.

Cracks in continuous deep beam tend to form before the negative cracks over the interior support, **Fig.2.3** shows the first significant cracking occurs in the form of diagonal shear cracks at about 50% of the ultimate load, the cracks tending to delineate a truss or tied arch mode of behavior. the expansion of the diagonal cracks is accompanied by the development and growth of additional secondary flexural cracks as the reinforcement is brought to yield, **Fig. 2.3**



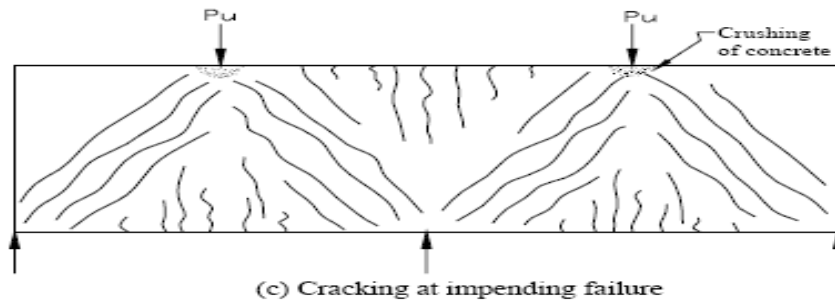


Fig.2.3 Cracks in beam due to excessive load.

Crack patterns and failure of deep beams have been observed under many different loading conditions. A single concentrated load, concentrated at the one-third points of the span and uniform loads. In these investigations deep beams were observed to fail in either shear or flexure. Although the load that caused the inclined crack was relatively independent of the a_v/d ratio, the ultimate strength increased as a_v/d decreased.

This was only true if the loads and reactions were on opposite faces of the beam so that a compression thrust could develop between the load and support. Load applied on the tension flange through a nib resulted in lower strengths than that load applied directly on the compression flange. Thus the ultimate shear stress in a beam without web reinforcement is approximately equal to the inclined cracking shear stress for members loaded at the tension flange and will be greater than the inclined cracking shear stress for directly loaded beams.

2.6. The importance of RC deep beams

It's known that the main parameters affecting the load bearing capacity of deep beams with or without web openings are shear span to depth ratio, configuration of web reinforcement, materials properties, and geometry of openings. Despite the rigorous studies of deep beams, there have been only empirical and semi-empirical formulas for predicting their ultimate load bearing capacities due to the complexities of the structural

nonlinearity and material heterogeneity. There have been also no pertinent theory and rational design code for predicting ultimate shear strength of reinforced concrete deep beams with web openings. Hence, it's very important and necessary that study of deep beams should be carried out experimentally and analytically to verify the shear of reinforced concrete deep beams which have various loading and geometric conditions.

2.7. The Need for Strengthening

There are several possible causes leading to the structural deficiency of existing infrastructure. Structural members can become damaged from environmental actions such as corrosion or freeze-thaw and excessive loading (static and dynamic) effects. The damaged concrete can be repaired with external or internal strengthening applied to supplement the lost capacity and improve environmental resistance. Improper detailing or damage during construction can necessitate the strengthening of newly constructed structural members.

Many researchers investigated on reinforced concrete deep beams, and most of them try to minimize the effect of shear in beams by normal reinforcement, so there few researches on the behavior for concrete deep members strengthened by CFRP with different shape and methods under concentrated load. To date, theoretical studies concerning the Carbon Fiber Reinforced Polymer (CFRP) and steel plate strengthening of RC deep beams have been rather limited. In addition, various numerical analyses presented so far have effectively simulated the behavior of solid beam strengthened by CFRP material.

2.8. The Importance of CFRP Polymers

Fiber-reinforced polymer (CFRP) has started to find its place in many areas of civil infrastructure applications where the need for repairing, increased durability arises...etc. also CFRP is used in civil structures where corrosion can be avoided at the maximum.

Fiber-reinforced polymer is better suited to minimize cavitation /erosion damage in structures such as sluice-ways, navigational locks and bridge piers where high-velocity flows are encountered. A substantial weight saving can be realized using relatively thin CFRP sections having the equivalent strength of thicker plain concrete sections. When used in bridges it helps to avoid catastrophic failures. Furthermore, in the quake prone areas the use of fiber-reinforced concrete would certainly minimize the human casualties. The amount of confining CFRP greatly affects the drift capacity of CFRP-retrofitted members.

The main disadvantage associated with the fiber-reinforced polymer is fabrication. The process of incorporating fibers into the cement matrix is labour-intensive and costlier than the production of the plain concrete. The real advantages gained using CFRP overrides this disadvantage ^{5}.

Fiber-reinforced polymers (CFRP) are currently emerging as a popular option to repair and strengthen reinforced concrete structures. This strengthening technique usually involves the bonding of a thin layer of FRP to the concrete surface of the structural element in need of repair. In order to fully develop the potential ductility of reinforced concrete flexural members, it is generally desirable that bending rather than shear governs the ultimate strength. However, shear deficiencies do often exist and in such cases there is a need for strengthening and retrofitting for increased shear capacities.

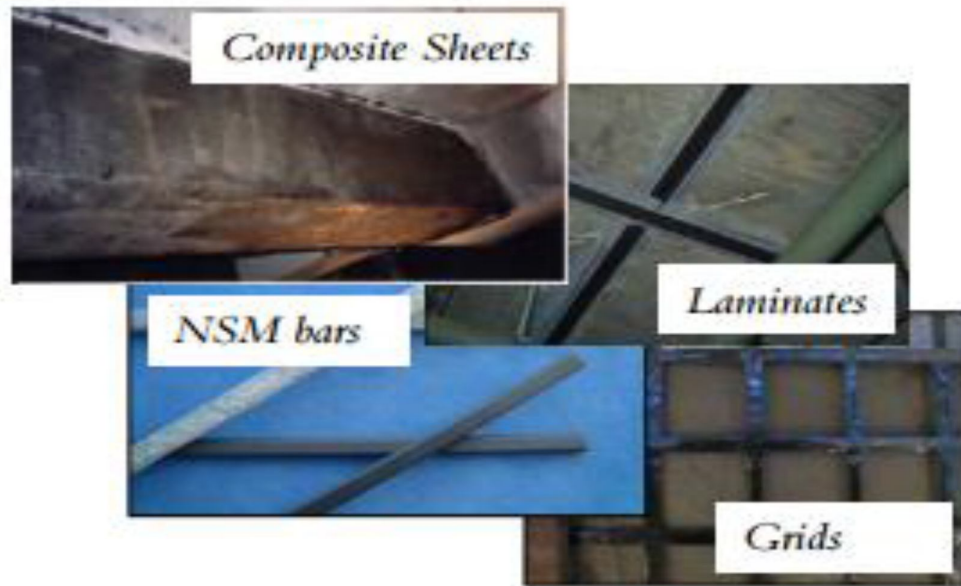


Fig.2.4. various composite materials.

2.8.1. CFRP Configuration

The failure mode of a strengthened beam depends also on the configuration of the strengthening used. From the configurations used the one to be avoided is the side bonded because it is the most exposed to debonding failure due to its limited anchorage length.

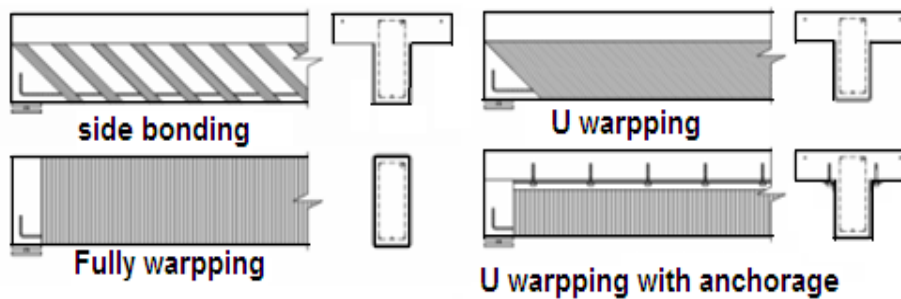


Fig. 2.5 Shear strengthening configurations using CFRP.

2.8.2. CFRP Orientations

For shear strengthening, CFRP can be applied in various configurations with different fiber orientation, degree of coverage, and type of

anchorage. The FRP can be applied as a continuous sheet along the length of a member or as discrete strips of prescribed minimum width and spacing. Maximum bond coverage is provided by sheets, whereas widely spaced strips provide the least degree of coverage {6}.

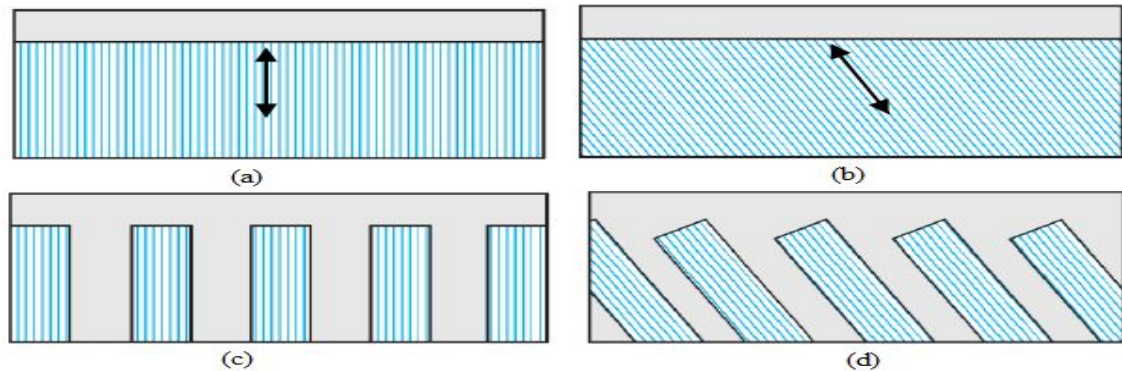


Fig. 2.6. Degree of FRP coverage and fiber orientation, (a) Sheet with fibers at 90° (b) Sheet with inclined fibers (c) Strips with fibers at 90° and (d) Inclined strips.

2.9. Failure mechanism of reinforced concrete beams.

In the case of flexural failure, the flexural cracks at the maximum bending moment location move toward the compression zone creating a hinge before failure. The curvature and the rotation at this location result in excessive deflection, providing a warning of impending failure. In the case of shear, the failure could occur due to diagonal tension or shear compression failure, and in both cases, the failure is much more brittle than the flexural failure.

2.9.1. Diagonal tension failure

This type of failure occurs in beams with a shear span ratio in the range of 2.5–5.5 **Fig.(2.7.a)**. Shear span is designed as the distance between the load and the support **Fig. (2.7.b)**. As the load increases, the region near the support where shear stresses are larger develops diagonal stresses that

could exceed the tensile strength of concrete. In some instances, small flexural cracks that are perpendicular to the axis of the beam could join the diagonal cracks. **Fig.2.7** Crack patterns and shear failure modes {38}

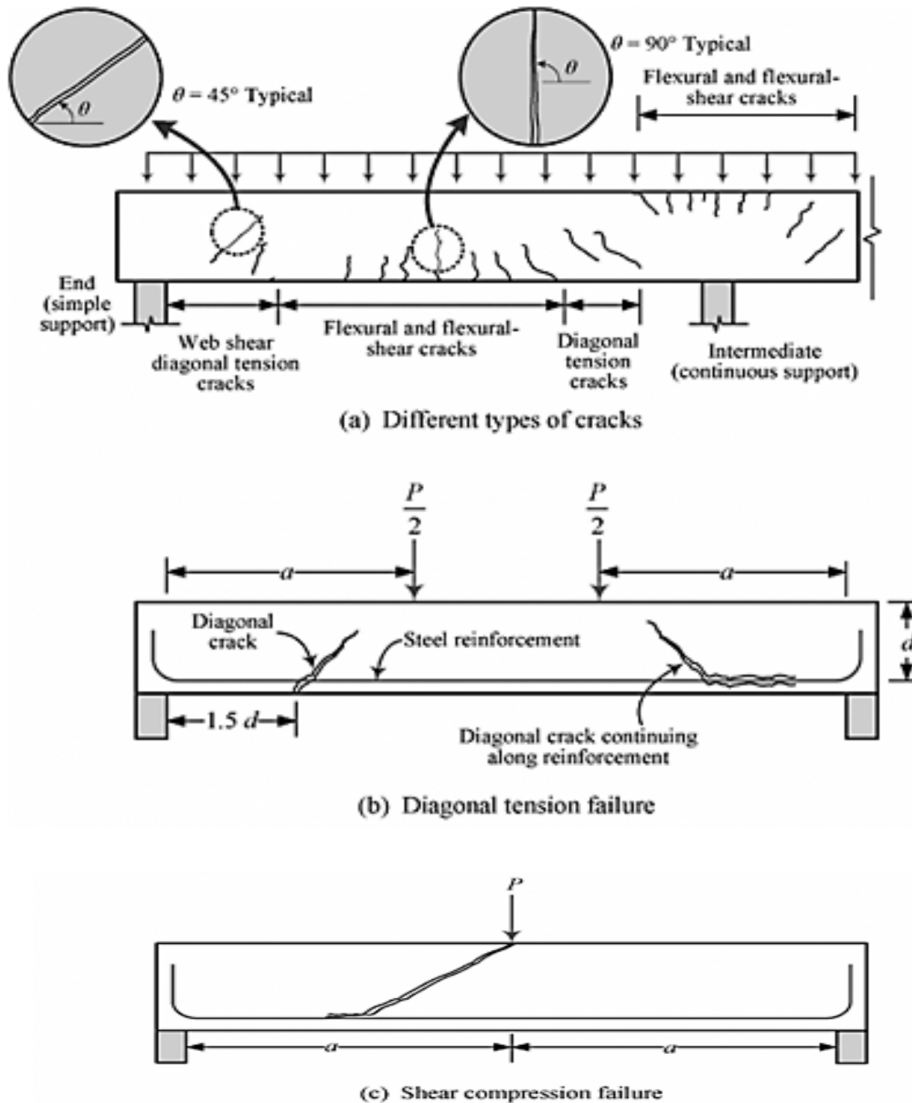


Fig.2.7. Crack patterns and shear failure modes{38}.

In some instances, the crack propagates along the reinforcement and could result in pull-out of the tension bar if the bar is not properly anchored. The critical location for diagonal cracks is between 1.5 and 2.5d from the support. The diagonal cracks, when occur at 45° to the axis of the beam; cover a distance of d along the axis. Owing to the presence

of normal (flexural) stresses, the angles of cracks do not exceed 45° . This is one of the reasons for limiting the maximum spacing of CFRP composites for stirrups to depth. This limit assures the presence of reinforcement at every diagonal crack. The same principle should be followed when designing shear reinforcement using composites. Diagonal shear cracks occur when the shear span-to-depth a/d ratio is between 2.5 and 5.5 for concentrated loads. If the ratio is less than 2.5, the mode of failure changes to shear-compression.

2.9.2. Shear compression failure

This type of failure occurs when the a/d ratio is less than 2.5 for concentrated loads, and 5 for distributed loads. These beams are typically referred to as deep beams. In this type of beam, the crack essentially travels from the load point to a location near the support -. The propagation is a result of both flexural and shear stresses. A system with fibers oriented in mutually perpendicular directions will provide an efficient reinforcement. The repair will also provide some confinement.

2.10. Previous experimental work

Nineteen small scale deep beams with depth varying from 178mm to 330mm and span of 610mm (span to depth ratios between 3.43 and 1.85) investigated by^[3]. From their work observations are as follows:

1. Neglecting effect on beams failing as a result of yield in the tension reinforcement.
2. Increasing the load capacity of beams failing in shear and in some cases if in changed the mode of failure from shear to flexural.
3. Increasing the amount of tension reinforcement increased the load capacity of the beams and tended to change the mode of failure from flexural to shear.

4. Increasing the depth (while holding the cross-section constant) increased the load capacity of beams failing in flexural, but did not show a proportional increase in shear strength.
5. The presence of web reinforcement did not appear to influence greatly the capacity beyond cracking for the beams regardless of the mode of failure.

Nine single span deep beams were tested having span to depth ratio of 1.0 and 0.9 respectively. The single span beams were uniformly loaded at their top and bottom chord while the two span beams were loaded on the top at the third points. Two additional single span deep beams having span to depth ratio of 1.67 were tested with the beam supported indirectly by adjoining deep beams. ^{7}

Leonhard suggested that the shear capacity of deep beams cannot be improved by the addition of the web reinforcement, apart later to be disproved by Kong and Robins who demonstrated that an increase in strength up to 30% is possible. Crack distributions and stress trajectories on top loaded beams with $L/D=1.0$, indicate that horizontal web reinforcement is helpful against the propagation of inclined cracks.

Kong and Robins carried out tests on simply supported lightweight concrete deep beams, and they developed a formula for calculating the ultimate load for normal weight concrete deep beams; it was found that this formula is not necessarily suitable for lightweight concrete beams. ^{8}

Further experimental work on lightweight concrete deep beams was reported by Kong and Robins (1972). They revised their previous formula in two factors: X_e/D ratio explicitly allowed for, and they used concrete cylinder splitting tensile strength (f_t), as they thought that the concrete contribution to the ultimate shear strength is much more directly related to tensile strength (f_t) than to the cylinder compressive strength (f_c).

Their tests showed that the ratio X_e/H had a greater effect on cracking and ultimate loads than L/H .

The proposed formula determined by ^{9} took into account the splitting strength of concrete and the influence of any steel crossing the failure crack, this suggestion for span/effective depth ratio less than one. It was stated that the failure of deep beams with small value of a_v/d ratio is analogous to the splitting of a cylinder along its length. The ultimate shear strength calculated by the proposed formula was found agree well with test results.

Several parameters such as shear span to depth ratio, the effect of horizontal and vertical reinforcement, and concrete strength were investigated by ^{10}. The following conclusion was drawn:

1. Beams generally failed in shear.
2. Minimum percentage of web reinforcement should be used for cracking control.
3. Inclined cracking occurs at approximately 50-60 % of the ultimate load.
4. Increasing the concrete strength increased the beams capacity.

Fifty-two simply supported reinforced concrete deep beams were tested under two symmetrical point loads. Considerable increase in load-carrying capacity was observed with increasing concrete strength and decreasing shear span-to-effective depth ratio. The increase in ultimate shear strength and in diagonal cracking load was attributed to the arch action for specimens with a shear span/depth ratio less than 2.5. It was also found that vertical stirrups became more efficient in beams with shear span/depth ratio less than 1.0. The effect of concrete strength was greater on beams with low shear span/depth ratio. Web reinforcement had no effect in controlling the diagonal cracking load and the cracking patterns were the same for beams with or without it. ^{10}

Seven reinforcement concrete wall panels with simply supported beams with depth/span ratio ranged from one to four are tested by ^{11}. They concluded that: The beam panel with depth/span ratio equal to 1.0 failed in shear with diagonal fracture line joining the load and support points, Beams with depth/span ratios greater than 1.0 failed by crushing of the bearing zones. This was the most common mode of failure among these members and was exhibited by panels with depth/span ratios between 1.5 and 3.5. The largest specimen tested, having a height/thickness ratio of 40, failed by buckling.

There are three modes of failure of deep beams have been demonstrated by ^{12} he tested thirteen simply supported reinforced deep beams with different span/depth ratio, and noted that the mode of failure are flexure failure, diagonal splitting failure and local crushing failure.

Nineteen reinforced concrete deep beams with high strength concrete were tested under two symmetrical top loading, with introduction of two main variables: shear span/depth ratio and span/depth ratio. The test results were compared with prediction based on ACI Building code. The comparison explained that the deep beam provisions in the ACI code though essentially based on concrete strength of less than 41Mpa, will insure safe designs for higher strength deep beams.

He reported experimental tests on twenty-two reinforced concrete deep beams with cylinder compressive strength of generally exceeding 55Mpa. Based on main steel ratio, ρ , the beams were organized into four groups with $\rho = 2.0, 2.58, 4.08,$ and 5.8 percent. The beams were tested for different a_v/d , ranging from 0.28 to 3.14. The comparison among the series was to highlight the influence of ρ and a_v/d ratio on the shear behavior of high strength concrete deep and short beams. It was shown that the transition point between high strength concrete (HSC) deep beams and high strength concrete shallow beams (in terms of load

carrying capacities) is around a_v/d of 1.5; for medium and low strength concrete beams, it was reported to occur between 2.0 and 2.5. The failure mode was chiefly influenced by the a_v/d ratio; the effect of ρ was not significant. For $a_v/d < 0.28$, the beams failed in bearing mode; for $0.28 < a_v/d < 0.12$, the beams failed in shear-compression mode; for $1.12 < a_v/d < 2.26$; the beams fail in diagonal tension mode and at $a_v/d = 2.5$; the beam failed in shear-Tension mode. For $a_v/d < 1.5$, increased the main tension steel ratio increases the load carrying capacities of HSC deep beams, but this beneficial effect was not as significant when $a_v/d > 1.5$. he also observed that the main reinforcement ratio greater than 2.0 percent did not increase the ultimate shear strength of HSC deep beams significantly. ^{13}

The effect of reinforced concrete deep beams size on shear capacity is studied by Hang Hai Tan et al. A total of 12 large and medium sized beams with overall height ranging from 1500 to 4520mm were tested under two symmetric point top loads to failure. The beams had compressive cylinder strength of about 40mpa. There was a pronounced effect of size on ultimate shear strength. The critical height beyond which there was no significant size effect was between 500 to 1000mm. However, the effect of size seems relatively independent of a_v/d .

The size effects for reinforced concrete beams strengthened in shear with CFRP strips were studied and tested by ^{14} and showed that the effective axial strains of the CFRP sheets are higher in the smaller specimens. Moreover, with a larger beam size, one can expect less strain in the CFRP. The performance of RC beams strengthened in shear by externally bonded U-shaped Carbon Fibre Reinforced Polymer (CFRP) wraps was suggested by ^{15}. Experimental results showed that externally bonded CFRP can increase the shear capacity of the beam significantly along

with improving the performance of strengthened RC beams. The Shear behavior of four full-scale deep beams reinforced with carbon and glass fiber reinforced polymer (CFRP) bars investigated by ^{16} . Their primary test variables included the longitudinal reinforcement ratio and the reinforcement type. The concrete compressive strength and reinforcement ratio had a clear effect on the ultimate capacity and deflection characteristics while reinforcement type no clear effect of the behavior of the tested beams. The results showed the necessity of the importance of considering the effect of axial stiffness on longitudinal reinforcement and including the effect of web reinforcement.

Four specimens investigated by ^{17}to study the shear strengthening of deficient reinforced concrete (RC) beams using carbon fiber-reinforced polymer (CFRP) sheets. The effect of the pattern and orientation of the strengthening fabric on the shear capacity of the strengthened beams were examined and his result obtained that the ultimate failure of strengthened beams occurred with delayed cracking of concrete eventually leading to the rupture of CFRP sheets and pulling of concrete on side and/or side cover delamination depending on the strengthening patterns.

The potential of using carbon fiber reinforced Polymer (CFRP) as reinforcement to concrete Beam was investigated by ^{18}. The CFRP reinforcement is applied in strip form, which is more economical compared to wrapping or forming it into bar shape, because it easier and uses less fiber to achieve similar performance. They concluded that the CFRP reinforced concrete beam give the required resistance and strength as designed, with behavior similar to those reinforced with steel bars. The understanding of the shear resisting mechanisms in RC beams shear-strengthened by externally bonded fiber-reinforced polymer (CFRP) sheets was illustrated by ^{19}. They analyzed and studied the effects of the

contribution of CFRP ratio on concrete, transversal steel strains and stresses, longitudinal tensile steel stresses, and diagonal compression struts and numerical results were compared with eight existing experimental results and the influence of the CFRP sheets on the shear strength of the beam. They concluded that the presence of CFRP reinforcement modifies the inclinations of cracks and struts and other parameters related to the shear response, producing great effects on the shear strength of the RC beams.

The I-shaped girders for ultrahigh performance fiber-reinforced concrete (UHPFRC) with varied types of shear reinforcement (stirrups and/or fibers, or neither), combined with longitudinal prestressed or mild steel reinforcing bars were studied by ^{20}. The contribution of the fibers to the shear response, prisms have been extracted horizontally, vertically, at 30 and 45° in both undamaged ends of the beams to determine the effective orientation factor was identified in this study. The efficacy of Carbon Fibre Reinforced Polymer (CFRP) strips in enhancing shear capacity and/or changing the failure mode from brittle shear failure to ductile flexural failure of RC beams. The results of the study indicate that while there is a marginal increase in first crack and ultimate loads, it is possible to achieve a change in the failure mode, and the monitored strain gauge data can be used to explain the failure pattern observed by ^{21}.

The torsional behavior of RC beams strengthened with externally bonded carbon fiber reinforced Polymer (CFRP) sheets, and to identify the influence of the investigated parameters affecting the torsional behavior on the effectiveness and feasibility of strengthening. And found that, the increase in the ultimate torsional moment for different strengthening configurations, performance improvement and crack patterns are presented^{22}. The shear resistance of RC beams strengthened with FRP

investigated by^{23}, they concluded that When the FRP reinforcement is in the form of U-jackets or side strips, debonding of the FRP reinforcement from the concrete substrate generally governs the shear strength of the beam and the evaluation of the shear resistance from the FRP becomes more challenging. An experimental study of large-scale (400 mm × 650 mm) beam specimens strengthened in shear with FRP was conducted to examine the effects of reversed cyclic loading and to quantify material shear strength contributions. The experimental research presented by ^{24} investigated the shear performance of rectangular reinforced concrete beams strengthened with CFRP U-strips as well as one completely wrapped with CFRP sheet; they observed that the larger beam size, CFRP sheet provided less improvement in the shear capacity. They investigated the cracking behavior of these specimens. Their research presented a Comparison between Test Results and Predictions from Design Guidelines.

Twelve specimens consisting of plain concrete beams, steel-reinforced concrete (SRC) beams, pure CFRP RC beams and hybrid CFRP RC beams were fabricated and tested. The test results show the hybrid CFRP RC beams behave in a more ductile manner when compared with the pure CFRP RC beams. Also, it is observed that a higher degree of over reinforcement in the beam specimen resulted in a more ductile CFRP RC beams. Hence, the addition of steel reinforcement can improve the flexural ductility of CFRP RC members, and over-reinforcement is a preferred approach in the design of CFRP RC members are tested by ^{25}. The performance of RC beams strengthened in shear by externally bonded U-shaped Carbon Fibre Reinforced Polymer (CFRP) wraps was presented by ^{15}. Different configurations of externally bonded U-shaped wraps were used to strengthen the beams in shear under four-point

bending with varying shear span-to-depth ratio (a/d). Experimental results showed that externally bonded CFRP can increase the shear capacity of the beam significantly along with improving the performance of strengthened RC beams.

The flexural behavior of carbon fiber reinforced polymer (CFRP) strengthened reinforced concrete (RC) beams determined by^{26}. For flexural strengthening of RC beams, total ten beams were cast and tested over an effective span of 3000 mm up to failure under monotonic and cyclic loads. The theoretical moment-curvature relationship and the load-displacement response of the strengthened beams and control beams were predicted by using FEA software ANSYS. Comparison has been made between the numerical (ANSYS) and the experimental results. The results show that the strengthened beams exhibit increased flexural strength, enhanced flexural stiffness, and composite action until failure.

The shear behavior of reinforced concrete beams strengthened by the attachment of different configurations and quantities of CFRP using epoxy adhesives investigated by^{27}. From experimental work clearly stated that moderate surface treatment for concrete before FRP bonding is sufficient to allow CFRP to do its job in a proper way.

the results of experimental and analytical studies on the flexural strengthening of reinforced concrete beams by the external bonding of high-strength, light-weight carbon fiber reinforced polymer composite (CFRP) laminates to the tension face of the beam are summarized by ^{28}.

The results indicate that the flexural strength of beams was significantly increased as the width of laminate increased. Theoretical analysis using a computer program based on strain compatibility is presented to predict the ultimate strength and moment-deflection behavior of the beams.

The experimental investigation on the response of continuous reinforced concrete (RC) beams with shear deficiencies, strengthened with externally bonded carbon fiber reinforced polymer (CFRP) sheets studied by {29}. The experimental results indicated that the contribution of externally bonded CFRP to the shear capacity of continuous RC beams is significant and is dependent on the tested variables. In addition, the test results were used to validate shear design algorithms. The proposed algorithms show good correlation with the test results and provided conservative estimates.

The results of an experimental and analytical study of the behaviour of damaged concrete beams retrofitted with CFRP sheets are presented by {30}. The effect of CFRP on strength of RC beams with different orientation is considered. Different modes of failure and gain in the ultimate strength were observed.

The shear behavior of reinforced concrete beams strengthened by the attachment of different configurations and quantities of CFRP using epoxy adhesives investigated{27}. Two types of CFRP materials were used. A general comparison between results is carried out showing the best configuration for strengthening.

2. 11. Previous analytical work on deep beams

The method of finite different to formulate equations to calculate shear and normal stresses for single span deep beams used by{31}. Although the method was directly applicable to structure mode of homogeneous materials. The stress distribution in such reinforced concrete members must be expected to, the non-homogeneity of the material; and the cracking of the tension zone. For this reason, no unique and strictly justified design procedure can be proposed.

Continuous deep beam is studied by ^{1} to analyze stress distribution and load arrangement. Many results were given for different load cases and different height/span ratio (H/L). These mathematical results were later used by Portland cement Association (1946) for the development of rules for concrete deep beam design.

The finite difference method also used by ^{31} to analyze the stress distribution. Single-span deep beams taken into consideration under five loading condition:

- One central concentrated load at the compression face.
- One central concentrated load at tension face.
- Uniform distributed load at compression face.
- Uniform distributed load at tension face and, finally two concentrated loads at third span on compression face.

Three height/span ratios were studied, 0.5, 1.0 and 2.0. It was observed that for all the types of loading, the stress curve agrees reasonably well with the linear distribution of the simple flexure theory when the height/span ratio was 0.5; as this ratio increased the difference between the linear distribution and the finite difference stresses become more significant. Three points of zero bending stress were noticed for height/span ratio equal to 2.0. Results from mathematical analysis under each loading case were provided in graphical form and it was pointed out that the stresses for any combination of loading could be computed by means of the principle of superposition. It was further suggested that these results could be used for the design of tensile and shear reinforcement of concrete deep beams and procedures for determining the amount of reinforcement required were given.

The tied-arch analytical method used by ^{33} to estimate a collapse load of deep beams with shear-span/effective-depth ratio of less than 1.0. It was summarized that the collapse load of the beams was determined by

investigating the failure of the member of the truss model, i.e. tension tie, inclined strut and horizontal arch rib. It was assumed that anchorage and bearing failures could be eliminated by adequate detailing.

It was assumed that shear crack is nearly straight line and hence the contribution of web reinforcement to the ultimate strength of deep beam was found. The equations of ultimate strength for both deep beams without web reinforcement and deep beam with web reinforcement was verified against the available tests results; good agreement was found.

that CFRP wraps to provide confinement to concrete, increasing its strength and ductility Shown by^{35}. They tested 55 R.C beams experimentally to study the effect of beam width, concrete strength, shear span-to-depth ratio, CFRP thickness, and strengthening configuration (completely wrapped, U-jacketing, and side bonding) in shear capacity of beams and used finite element programming (ANSYS) to verify the results.

An improved analytical method is used by ^{36} to predict the deflection of rectangular reinforced concrete beams strengthened byC FRP composites applied at the bottom of the beams. He was concluded that results obtained from the energy variation method show very good agreement with results obtained from the finite element method.

2.12. Traditional methods and Codes of Practices for Calculating RC Beams Capacity

As a result, some proposals or recommendations have been adopted in different countries for the design of reinforced concrete structures reinforced or strengthened with FRP sheets, such as ACI 440 (2005), Triantafillou and Antonopoulos (2000) Matthys and Triantafillou (2001), Carolin and Taljsten (2005a), and Zhang and Hsu (2005).

ACI Codes:

Beams without opening: the ACI code (1995, 2005) suggested two alternative methods:

a- Detailed method:

The detailed method makes an attempt to include the effect of concrete strength, dowel action of longitudinal reinforcement bars, and the moment-to-shear ratio at the section on ultimate shear strength. The equation predicting the shear strength of a beam is given as

$$V_c = \frac{1}{6} \left[\sqrt{f'_c} + 100 \frac{\rho_w V_u d}{M_u} \right] b_w d \leq 0.3 \sqrt{f'_c} b_w d \quad (2.1)$$

Where V_u =factored shear force; M_u =factored moment; ρ_w =reinforcement ratio; b_w =web width; and d = effective depth; and $\frac{V_u d}{M_u}$ shall not greater than 1.0.

b- Simplified method: the above equation is not so simple to use as a design equation, the ACI code permits use of below equation:

$$V_c = \frac{1}{6} \sqrt{f'_c} b_w d \quad (2.2)$$

For values of ρ_w smaller than 0.0012, the following equation is suggested

$$V_c = (0.07 + 8.3 \rho_w) \sqrt{f'_c} b_w d \quad (2.3)$$

For beams with shear reinforcement, the ACI consider nominal shear strength, V_n as flow:

$$V_n = V_c + V_s \quad (2.4)$$

Where V_c = shear strength of concrete; V_s = shear strength of shear reinforcement.

Shear strength for inclined stirrup at an angle α with horizontal suggested as:

$$V_s = \frac{A_v f_{yv} (\sin\alpha + \cos\alpha) d}{s} \quad (2.5)$$

Where A_v , f_{yv} are area of shear reinforcement in distance s and yield strength of shear reinforcement respectively.

When $\alpha = 90^\circ$ (vertical stirrups are used) the above equation reduces to

$$V_s = \frac{A_v f_{yv} d}{s} \quad (2.6)$$

$$\text{but } \phi V_s \geq V_u \quad (2.7)$$

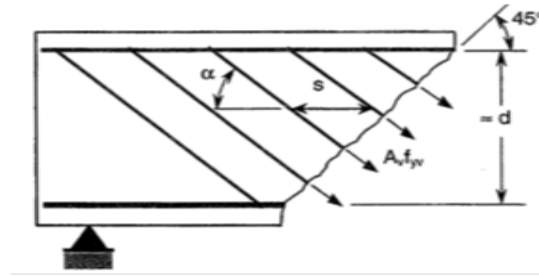


Fig.2.8. shear strength vs. provided by shear reinforcement

Minimum shear reinforcement, maximum stirrup spacing and maximum shear were provided from following equations respectively:

$$\left[\frac{A_v}{s} \right]_{\min} = \frac{1b_w}{3f_{yv}} \quad (2.8)$$

$$S_{max} = \frac{d}{4} \leq 600\text{mm, when } 0.5\phi V_c < V_u \leq 3\phi V_c \text{ and}$$

$$S_{max} = \frac{d}{4} \leq 300\text{mm, when } 3\phi V_c < V_u \leq 5\phi V_c \quad (2.9)$$

$$[V_u]_{\max} = 5\phi V_c = \frac{5}{6} \phi \sqrt{f'_c} b_w d \quad (2.10)$$

Formulations for the shear resistance of external CFRP sheets bonded to a rectangular beam are often described differently by various researches and design guidelines. Most are in fact based on the same equation that incorporates beam geometry, CFRP geometry, and CFRP effective strength or strain. This basic equation for the un-factored shear resistance attributed to CFRP can be expressed in the following form ^{37}:

$$V_u = f_{fe} \rho_{uf} b_w d_f (\cot \theta + \cot \beta_f) \sin \beta_f \quad (2.11)$$

Where ρ_f = the FRP reinforcement ratio, b_w = the beam web width, f_{fe} = the FRP effective stress in the principal fiber direction, and θ = the principal compressive stress inclination. The FRP effective stress is defined as the effective strain multiplied by the modulus of elasticity, E_f . The term β_f = the angle of the FRP principal tensile fibers, measured with respect to the member longitudinal axis. The term d_f = the effective depth of the FRP, the definition and calculation of which varies by code, and is sometimes presented as the effective height, h_{fe} . The FRP reinforcement ratio is defined as follows:

$$\rho_f = \left(\frac{A_f}{S_f b_w} \right) = \left(\frac{2t_f w_f}{S_f b_w} \right) \quad (2.12)$$

A_f is calculated as the total CFRP thickness on both beam web faces multiplied by the width of a CFRP strip, w_f .

CHAPTER THREE

**MATERIALS PROPERTIES
AND SUMMARY OF DESIGN
EQUATIONS FROM VARIOUS
GUIDELINES**

CHAPTER THREE

MATERIALS PROPERTIES AND SUMMARY OF DESIGN EQUATIONS FROM VARIOUS GUIDELINES

3.1 General

Based on this study, a prediction model was proposed by considering all common parameters that influence the ultimate shear capacity of a strengthened beam including concrete strength (f'_c), effective height of the beam (d), FRP thickness (t_f), and strengthening configuration (completely wrapped, U-jacketing, and side bonding).

The obtained results were compared with that recommended design guide given by the code (ACI code). Beam geometry was illustrated in Fig. (3.7)

3.2. Comparison of different method with Design Guidelines

Following the previous discussion on the behavior of CFRP shear-strengthened beams, it is of interest to see how the measured shear capacity compares with the predictions from available design guidelines. Three design guidelines are considered in this study which compared with American Concrete Institute (ACI) (2008) such as Triantafillou and Anton 2000, carolin and Taljsten 2005 and Zhichao and Cheng 2005.

The equations used in this part of this study related with below guides:

3.2.1. ACI equation

(a) Simplified method: the equation (2.1) is not so simple to use as a design equation, the ACI code permits use of below equation:

$$V_c = \frac{1}{6} \sqrt{f'_c} b_w d \quad (3.1)$$

For beams with shear reinforcement, the ACI consider nominal shear strength, V_n as flow:

$$V_n = V_c + V_s \quad (3.2)$$

Which V_c = shear strength of concrete; V_s = shear strength of shear reinforcement.

Shear strength for inclined stirrup at an angle α with horizontal suggested as:

$$V_s = \frac{A_v f_{yv} (\sin\alpha + \cos\alpha) d}{s} \quad (3.3)$$

Which A_v , f_{yv} are area of shear reinforcement in distance s and is the yield strength of shear reinforcement respectively.

When $\alpha = 90^\circ$ (vertical stirrups are used) the above equation reduces to

$$V_s = \frac{A_v f_{yv} d}{s} \quad (3.4)$$

$$\text{but } \phi V_s \geq V_s \quad (3.5)$$

The nominal shear strength of an CFRP-strengthened concrete member can be determined by adding the contribution of the CFRP external shear reinforcement to the contributions from the reinforcing steel (stirrups, ties, or spirals) and the concrete. An additional reduction factor ψ_f is applied to the contribution of the CFRP system.

$$\phi V_n = \phi (V_c + V_s + \psi_f V_f) \quad (3.6)$$

The reduction factor ψ_f of 0.85 is recommended for the three-sided CFRP U-wrap or two-opposite-sides strengthening schemes. Insufficient experimental data exist to perform a reliability analysis for fully-wrapped sections; however, there should be less variability with this strengthening scheme as it is less bond independent, and therefore, the reduction factor ψ_f of 0.95 is recommended.

Fig.3.1 illustrates the dimensional variables used in shear-strengthening calculations for CFRP laminates. The contribution of the CFRP system to shear strength of a member is based on the fiber orientation and an assumed crack pattern. The shear strength provided by the CFRP

reinforcement can be determined by calculating the force resulting from the tensile stress in the CFRP across the assumed crack. The shear contribution of the FRP shear reinforcement is then given by:

$$V_f = A_{fv} f_{fe} (\sin\alpha + \cos\alpha) d_{fv} / s_f \quad (3.7)$$

Where: $A_{fv} = 2 n t_f w_f$

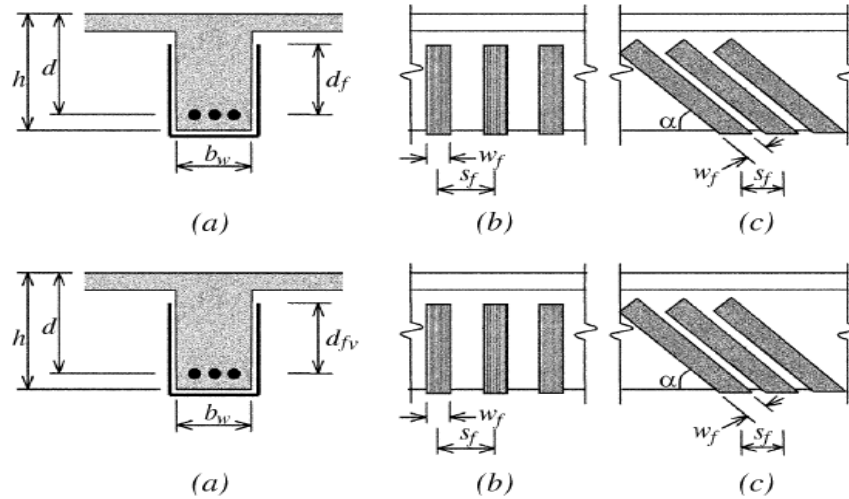


Fig. 3.1. Illustration of the dimensional variables used in shear-strengthening calculations for repair, retrofit, or strengthening using CFRP laminates.

The effective strain is the maximum strain that can be achieved in the CFRP system at the nominal strength and is governed by the failure mode of the CFRP system and of the strengthened reinforced concrete member. The licensed design professional should consider all possible failure modes and use an effective strain representative of the critical failure mode. The following subsections provide guidance on determining this effective strain for different configurations of CFRP laminates used for shear strengthening of reinforced concrete members.

For reinforced concrete column and beam members completely wrapped by CFRP

$$\epsilon_{fe} = 0.004 \leq 0.75\epsilon_{fu} \quad (3.8)$$

CFRP systems that do not enclose the entire section (two- and three-sided wraps) have been observed to delaminate from the concrete before the loss of aggregate interlock of the section. For this reason, bond stresses have been analyzed to determine the usefulness of these systems and the effective strain level that can be achieved. The effective strain is calculated using a bond-reduction coefficient κ_V applicable to shear:

$$\varepsilon_{fe} = \kappa_V \varepsilon_{fu} \leq 0.004 \quad (3.9)$$

The bond-reduction coefficient can be computed from:

$$\kappa_V = \frac{k_1 k_2 L_e}{111,900 \varepsilon_{fu}} \leq 0.75 \quad (3.10)$$

The active bond length L_e is the length over which the majority of the bond stress is maintained. This length is given by:

$$L_e = \frac{23300}{(n_f * t_f * E_f)^{0.58}} \quad (3.11)$$

L_e bond-reduction coefficient also relies on two modification factors, k_1 and k_2 , that account for the concrete strength and the type of wrapping scheme used, respectively. Expressions for these modification factors are given in

$$k_1 = \frac{(f_c)^{0.67}}{27} \quad \text{in SI units} \quad (3.12)$$

$$k_2 = \frac{df_v - L_e}{df_v} \quad \text{for U- wraps} \quad (3.13)$$

$$k_2 = \frac{df_v - 2L_e}{df_v} \quad \text{for two side bonded} \quad (3.14)$$

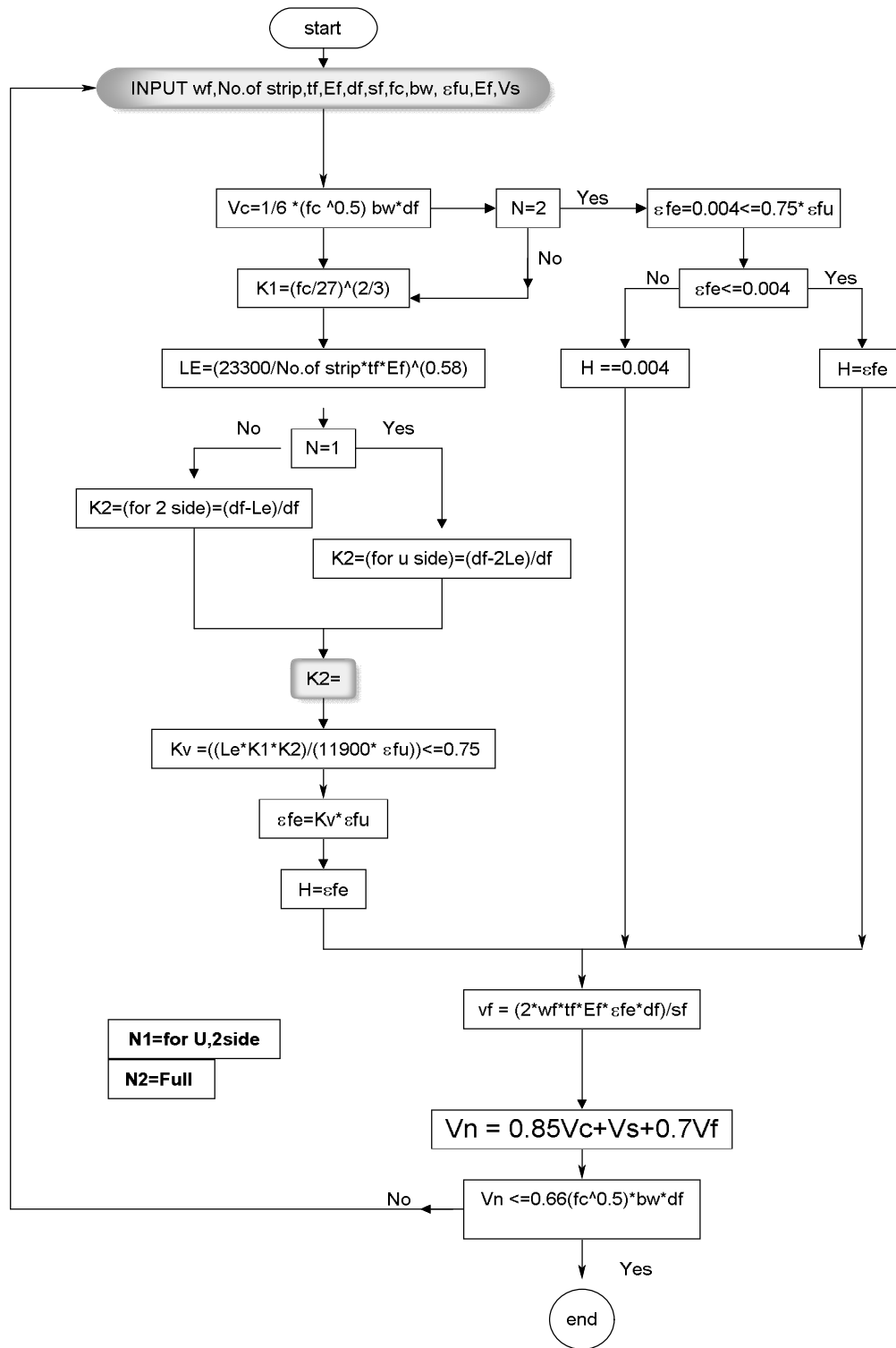


Fig.3.2. Flow chart of (ACI) method

3.2.2. Triantafillou and Anton 2000 equation for FRP contribution

In the deterministic approach, based on an analysis (curve fitting) of a large data base of experimental results, equations for the effective strain are proposed as a function of a correlation parameter. Triantafillou (1997, 1998) argues effective strain level in FRP reinforcement attained at failure (ϵ_{fe}) will mainly depend on the available development length of the FRP (Force transfer zone at both sides of the shear crack) which is a function of the bond conditions and the FRP axial rigidity (area time elastic modulus). By means of an experimental data fitting, it is proposed to calibrate $\epsilon_{f,eff}$ as a function of $E_f p_{wf}$, with $p_{wf} = (A_w f / (s_f * b w))$.

Here with, the CFRP shear contribution V_f, exp is taken as the difference between the experimental failure load of the strengthened beams. Given $V_f, experimental$. and assuming diagonal shear cracks with $\theta = 45^\circ$.

According to this approach a relationship for Corresponding strain $\epsilon_{f,eff}$ is suggested by Triantafillou (1997,1998), later on ,this was updated (Triantafillou and Antonopolos,2000), .A similar approach by Khalifa et al (1998) the curves are plotted against test results of 70 experiments. The latter database, collected by Matthys (2000), comprises the original data found in the literature. Based on this data Matthys (2000), proposed relationships from recreation with ϵ_{fe} as a function of:

$$\epsilon_{fe} = 0.17 \left(\frac{(f_c)^{0.67}}{E_f * P_f} \right)^{0.3} * \epsilon_{fu} \text{ for full wrap} \quad (3.15)$$

$$P_f = \frac{2W_f * t_f}{b * s_f} \quad (3.16)$$

$$\epsilon_{fe} = 0.72 * \epsilon_{fu} * e^{-(0.0431 * \Gamma_f)} \text{ for 2 or 3 side wrap} \quad (3.17)$$

$$\Gamma_f = \left(\frac{E_f * P_f}{(f_c)^{0.67} * \left(\frac{a}{d}\right)} \right) \quad (3.18)$$

With (a/d) the shear span to effective depth ratio.

$$v_f = \frac{2W_f * t_f * E_f * \epsilon_{fe} * d_f}{s_f} \quad (3.19)$$

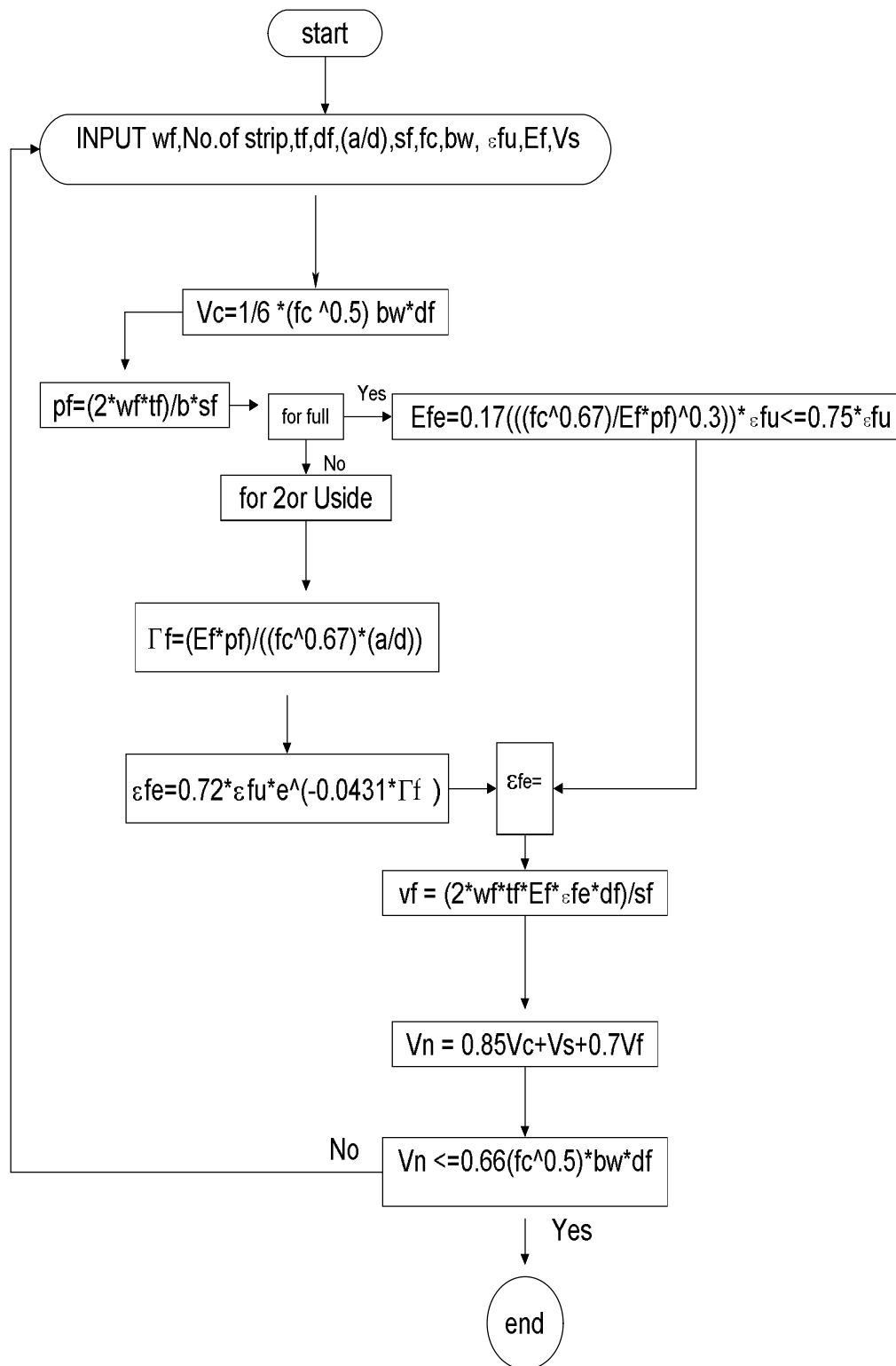


Fig.3.3. Flow chart of Triantafillou and Anton method.

3.2.3. Carolin and Taljsten 2005 equation

(η) average fiber utilization. The average fiber utilization expresses the average strain in the fiber over the height compared to strain in the most stressed fiber ϵ_{\min} in cross section.

Fiber bonded vertically, with stiffness only in that direction, are not affected by the bending moment and fiber utilization, is 0.6, this value obtain from 70 specimens tested by carolin

Carolin suggest that the derivation of fiber contribution based on the truss theory requires a definition of an arbitrary path of a possible shear crack. This shear crack is assumed to follow the compression strut in the concrete and to open in the perpendicular direction. Fibers bonded over this possible crack will become stressed by the crack opening and then give a contribution to the shear capacity of the beam. When plate bonding is used for strengthening, the direction of the principal stresses may be predicted with high accuracy and the fiber can be placed in the most effective direction. However, the direction of the shear crack is difficult to foresee, and the principal strains and stresses will only in exceptional cases coincide with the fiber direction. Therefore, three geometric angles are needed in the following analysis Fig. (3.4). The angle (α) for crack inclination, β for fiber direction in relation to the beam's longitudinal axis, and ϕ for angle between the principal tensile stress and fiber direction. That is $\phi = \alpha + \beta - 90$.

The contribution from the composite, V_f can be described as

$$V_f = F_f * \sin \beta \quad (3.20)$$

where $F_f = \Sigma F_n$

And F_n is the force in each composite strip over the assumed crack and is calculated as

$$F_f = \sigma_f e * A_f \quad (3.21)$$

In Eq. (3.21) the effective stress, σ_{fe} can be calculated by Hook's law and stiffness only in fiber direction

$$\sigma_{fe} = \epsilon_{fe} * E_f \quad (3.22)$$

In equ. (3.22) the effective strain ϵ_{fe} , can be calculated as

$$\epsilon_{fe} = \eta \epsilon_{cr} \quad (3.23)$$

Where z is the length of a vertical tension ties in the truss, for steel stirrups normally expressed by the internal lever arm or $0.9d$. For composites bonded over the whole height, z becomes equal to the beam height, h . For laminates, the thickness, t_f .

The factor (r_f) depends on the strengthening scheme and becomes b_f/s_f . The value of (η) is based on the analysis, suggested to be (0.6). The final equ. is:

$$V_f = \frac{\eta * \epsilon_{cr} * E_f * t_f * r_f * z * \cos \phi}{\sin \alpha} \quad (3.24)$$

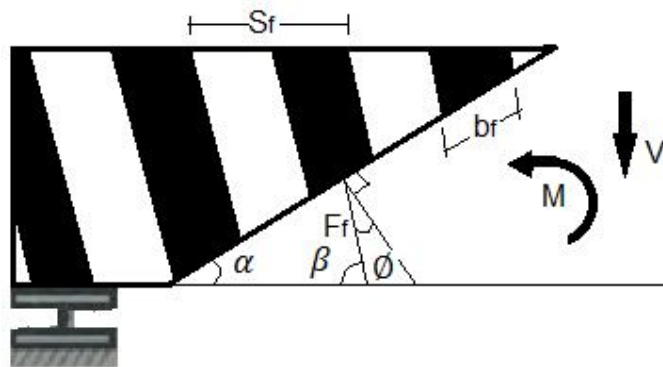


Fig. 3.4 Illustration of the (β, ϕ, α)

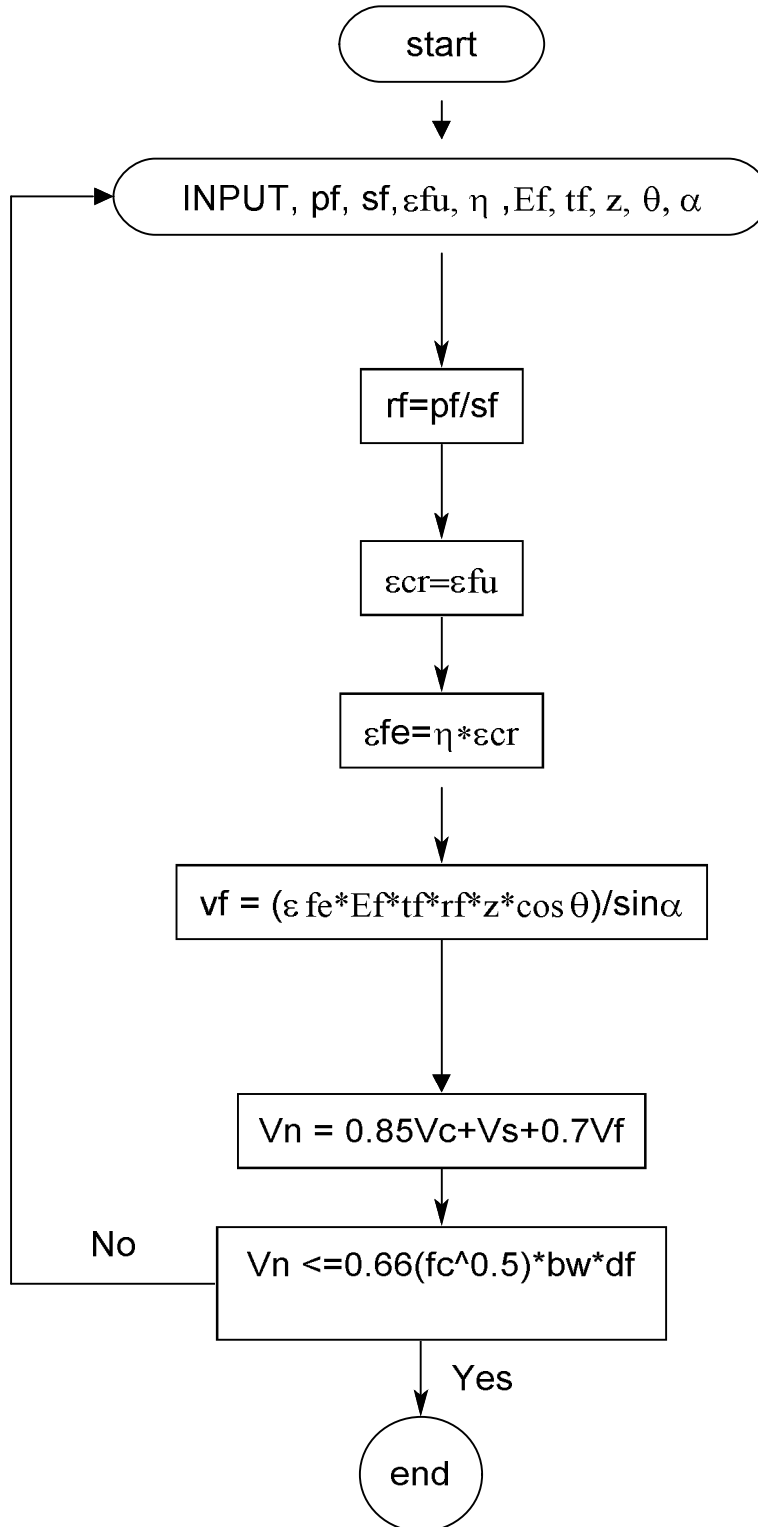


Fig.3.5.Flow chart for carolin and Taljsten 2005 method.

3.2.4. Zhichao and Cheng 2005 equation

$$V_f = \frac{(A_{fe})(A_f \sin B + \cos B) * E_f * \epsilon_{fe} * d_f}{s_f} \quad (3.25)$$

$$A_{fe} = 2W_f * t_f \quad (3.26)$$

In Eq. (3.26). A_f is the area of CFRP shear reinforcement, B is the angle between the orientation of the principal fibers in the CFRP laminates and the longitudinal axis of the beam, d_f is the effective depth of the CFRP laminates, s_f is the CFRP strip spacing, E_f the elastic modulus of CFRP laminates and ϵ_{fe} is tensile strain of CFRP laminates when the beam failed in shear.

To apply equ.(3.25), (V_f) necessary to find the actual value of the effective strain ϵ_{fe} . Since the ultimate tensile ϵ_{fu} of CFRP laminates can be obtained from material properties provided by the manufacturer, a reduction factor R is needed to calculate the effective strain ϵ_{fe} .

$$\epsilon_{fe} = R \epsilon_{fu} \quad (3.27)$$

Thus, the R -value becomes the most important parameter in determining the shear contribution of CFRP. In this research, three approaches are presented to determine the R -value, and be used to calculate the effective strain.

R-Value Based on Model Calibration

Triantafillou (1998) observed that the effective strain is a function of the axial rigidity of the FRP sheet, which is $p_f E_f$, where p_f is the CFRP shear reinforcement ratio. The implication of this argument is that the effective FRP strain decreases as the FRP laminates become stiffer and thicker. Thus, the effective strain versus the axial rigidity can be found by curve fitting. Since the database used includes various kinds of FRP sheets, Khalifa et al, (1998) suggested that the ratio of effective strain to ultimate strain $R = \epsilon_{fe} / \epsilon_{fu}$ be plotted against axial rigidity $p_f E_f$,

Khalifa et al, (1998) presented two equations to calculate R, one for CFRP rupture and another for delamination of CFRP from the concrete surface. The smaller R calculated from three equations will be used. The three equations are listed below

$$R = 0.5622(Pf * Ef)^2 - 1.2188(pf * Ef) + 0.778 \quad (3.28)$$

Although Eq.(3.28) Above is calibrated from the test results of both CFRP rupture and delamination, Khalifa et al, (1998) claimed it should only be used to calculate the reduction factor for rupture. In this equation, pf is the CFRP shear reinforcement ratio, which is defined as

$$2 * tf * wf / (bw * sf) \quad (3.29)$$

W_f = CFRP strip width; bw = cross-section width of the RC beam; and s_f = CFRP strip spacing

$$R = (0.0042(f_c)^{0.67} * wf) / (Ef * tf)^{0.58} * \epsilon_{fu} * df \quad (3.30)$$

Eq. (3.30) above which is derived from analysis done by Khalifa et al.(1998), has been used to calculate the reduction factor for CFRP delamination from concrete surface. In this equation, W_f is defined as the effective width of CFRP sheets.

$$R = 1.8589 \left(\frac{Ef * Pf}{f_c} \right)^{-0.7488} \quad (3.31)$$

Considering that Eq. (3.31) Above is based on a regression line and that the data points are not distributed right on it, a safety factor should be applied to the equation to account for the data points below the line curve, the curve for modified is well below most of the data points equ.(3.31) Above can then be transformed to equ.(3.32) Below after multiplying a safety factor of 0.8, (0.8 = r-squared value from curve points)

$$R = 1.4871 \left(\frac{Ef * Pf}{f_c} \right)^{-0.7488} \quad (3.32)$$

use (R) Which is small

$$V_f = \frac{2W_f * t_f * E_f * \epsilon_{fe} * d_f}{s_f} \quad (3.33)$$

$$P_f = \frac{2W_f * t_f}{b * s_f} \quad (3.34)$$

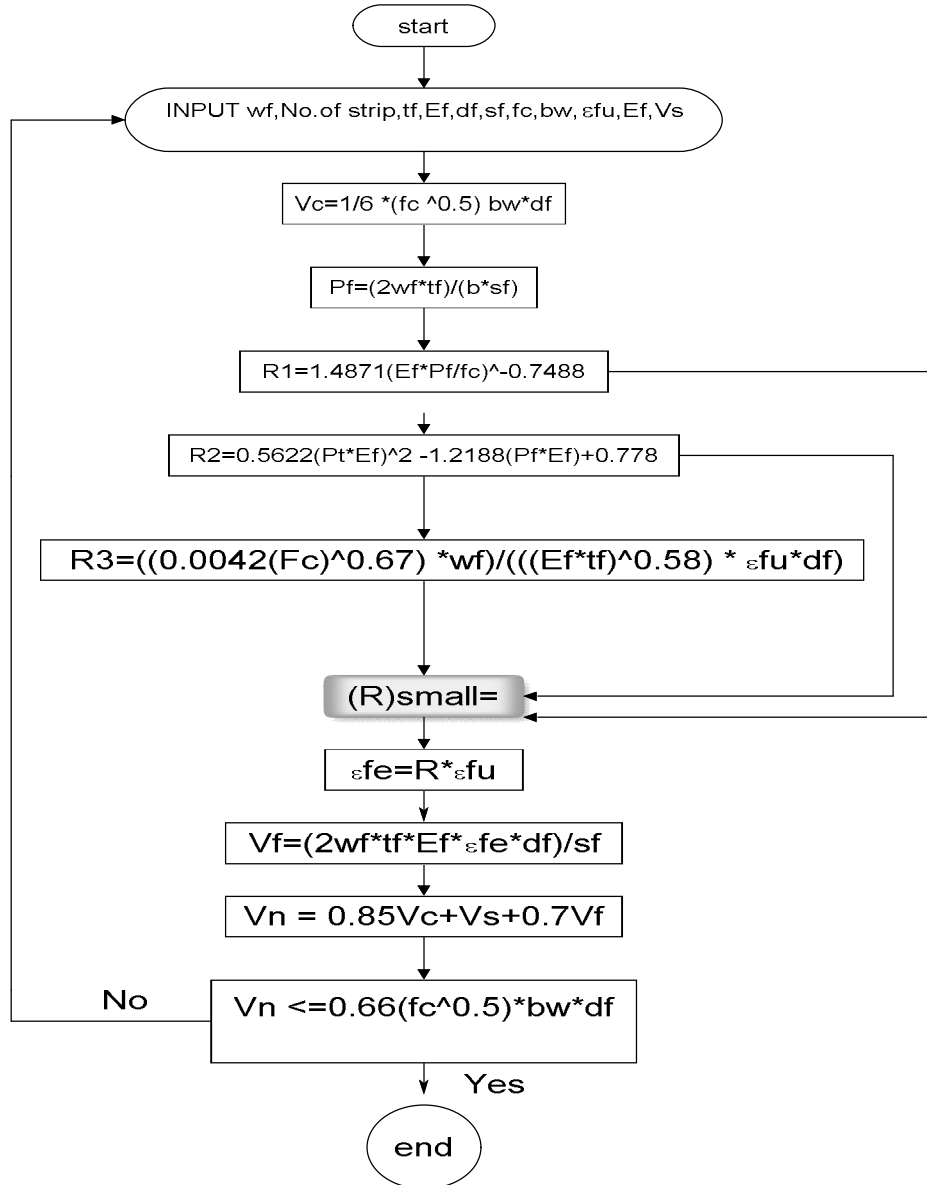


Fig.3.6. Flow chart of Zhichao and Cheng.

3.3. Material properties and codes of practice used in this study

The parameters considered in this study are: the shear span to effective depth ratio, the width, the effective depth, the height to width ratio, effective span to depth ratio, strength of concrete, strength N of main reinforcement, main reinforced ratio, vertical web reinforcement ratio and horizontal web reinforcement ratio. properties of materials used in **Table 3.1** and Geometrical details of proposed RC beams **Fig.3.7**

Table 3.1 the materials properties of Deep beam

Specified yield strength of nonprestressed steel reinforcement, (F_y)	420(MPa)
Width of FRP reinforcing plies, (W_f)	100(mm)
specified compressive strength of concrete, (f_c')	28(MPa)
tensile modulus of elasticity of FRP, (E_f)	223500(MPa)
Distance between Center to Center(two plies of CFRP)	200(mm)
overall thickness or height of a member, (h)	1200 (mm)
design rupture strain of FRP reinforcement, (ϵ_{fu})	0.018(mm/mm)
design ultimate tensile strength of CFRP, (f_{fu})	3000(MPa)
No. of FRP reinforcing plies	2
width of a member, (b)	250(mm)

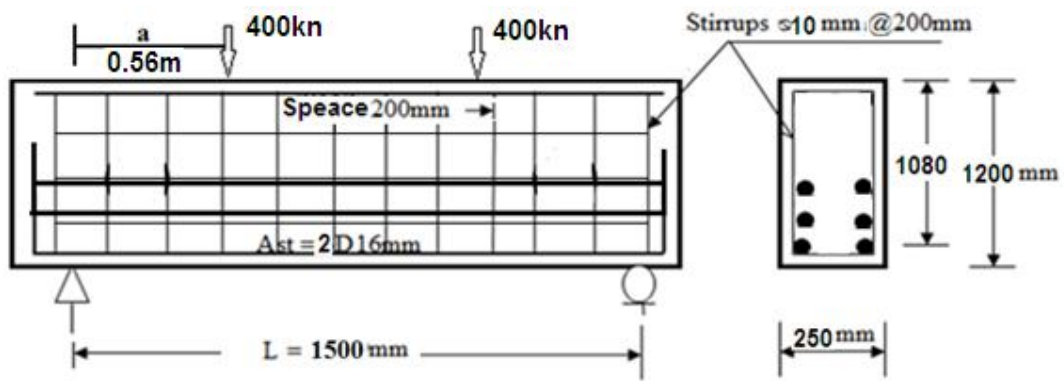


Fig. 3.7 Geometrical details of proposed RC beams.

CHAPTER FOUR

RESULTS AND DISCUSSION

CHAPTER FOUR

RESULTS AND DISCUSSION

4.1 Introduction

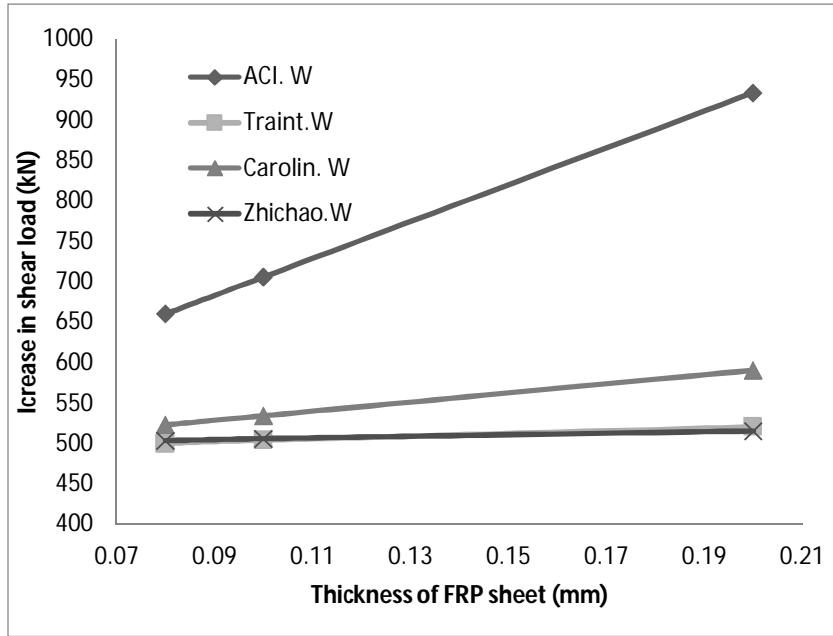
The main goal for this work was to study the influence of fiber reinforcement polymer (CFRP) on shear behavior of deep beams with various guidelines. The purpose was also to study the strength parameters such as, FRP thickness, beam depth and concrete COMPRESSIVE strength. The design of shear strength were prepared by Microsoft Excel spread sheet for three configuration of wrapping to study the effect of deferent parameter on shear capacity of deep beams.

4.2. Effect of FRP Thickness on Shear Strength of RC Deep beams.

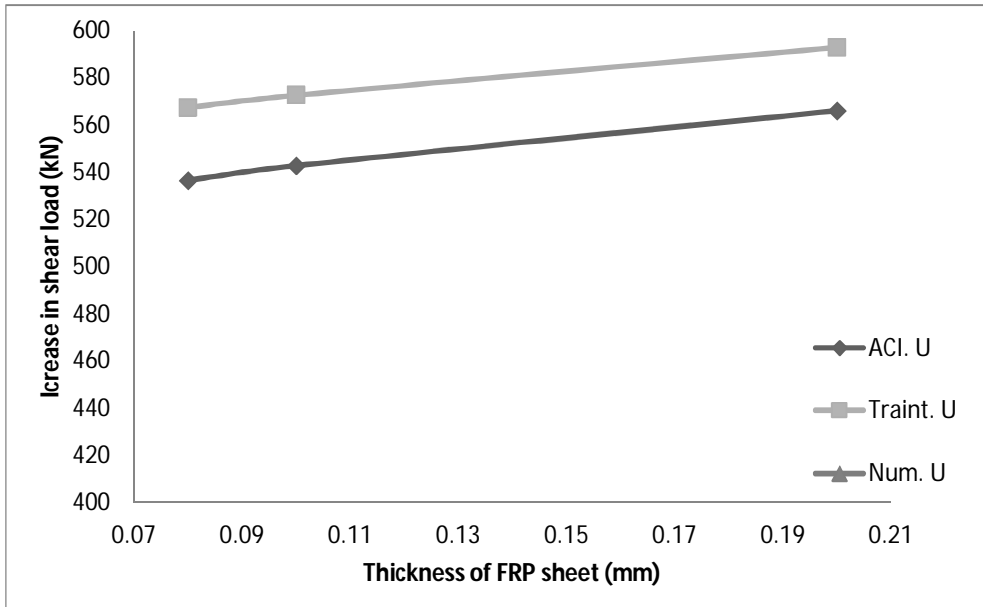
It was a clear that FRP thickness has greater effect on shear strength as shown in **Fig. 4.1** and **Table 4.1**, Thickness of FRP ,which consider was (0.08mm),(0.1mm),(0.2mm) for different configuration.

**Table 4.1 The influence of FRP thickness on shear capacity (kN)
using different method.**

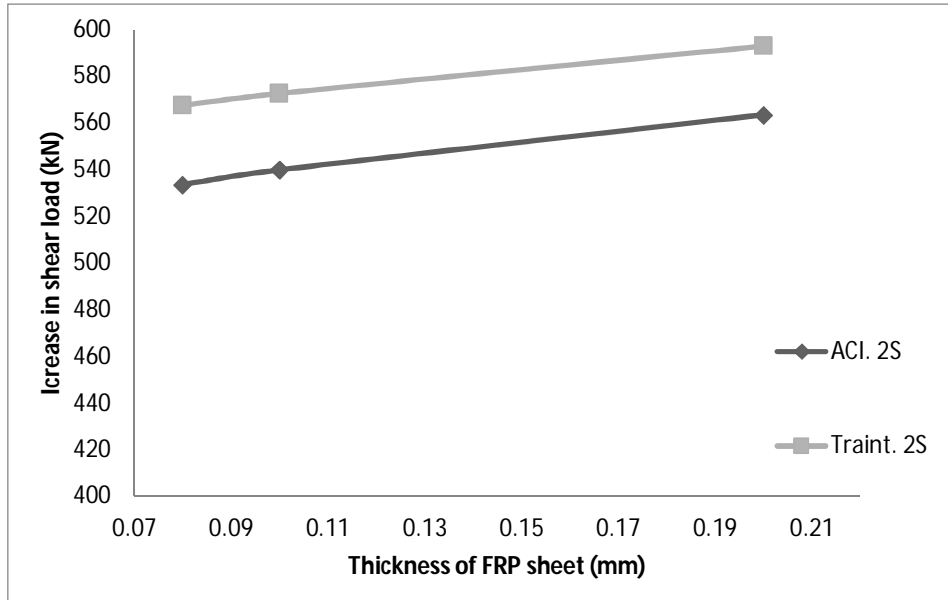
Configu- ration	FRP thickness	ACI	Trianta- fillou	Carolin	Zhichao	Percentage Of Different		
						Trianta- fillou	Carolin	Zhichao
Full warping	0.08mm	660.1	500.0	522.7	503.2	24.2%	20.8%	23.7%
	0.1mm	705.8	503.8	534.03	505.7	22.2%	24.3%	28.3
	0.2mm	933.9	520.1	590.4	515.2	44.3%	36.7%	44.8%
U- shape	0.08mm	536.6	567.4	-	-	-5.7%		
	0.1mm	542.8	572.6	-	-	-5.6%		
	0.2mm	566.1	592.9	-	-	-4.7%		
Two side	0.08mm	533.5	567.4	-	-	-6.3%		
	0.1mm	539.8	572.6	-	-	-6.1%		
	0.2mm	563.4	592.9	-	-	-5.2%		



(a)



(b)



(c)

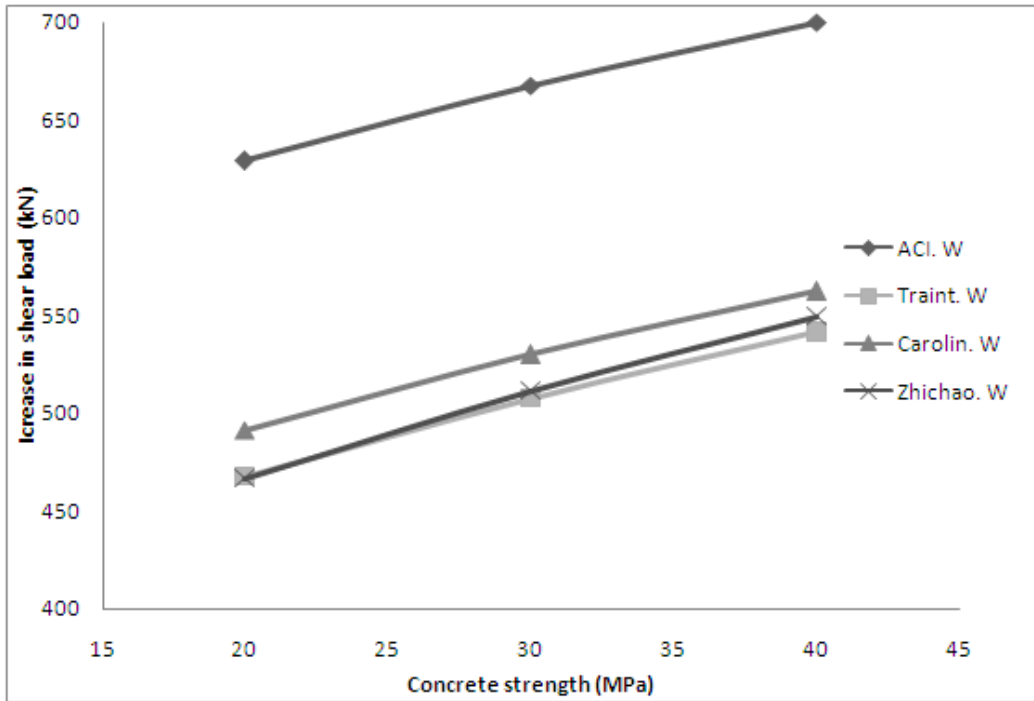
Fig. 4.1. Effect of FRP thickness on concrete shear strength for different guidelines (a) full wrap (b) U wrap (c) two sides.

4.3. Effect of Concrete Strength on Beams capacity

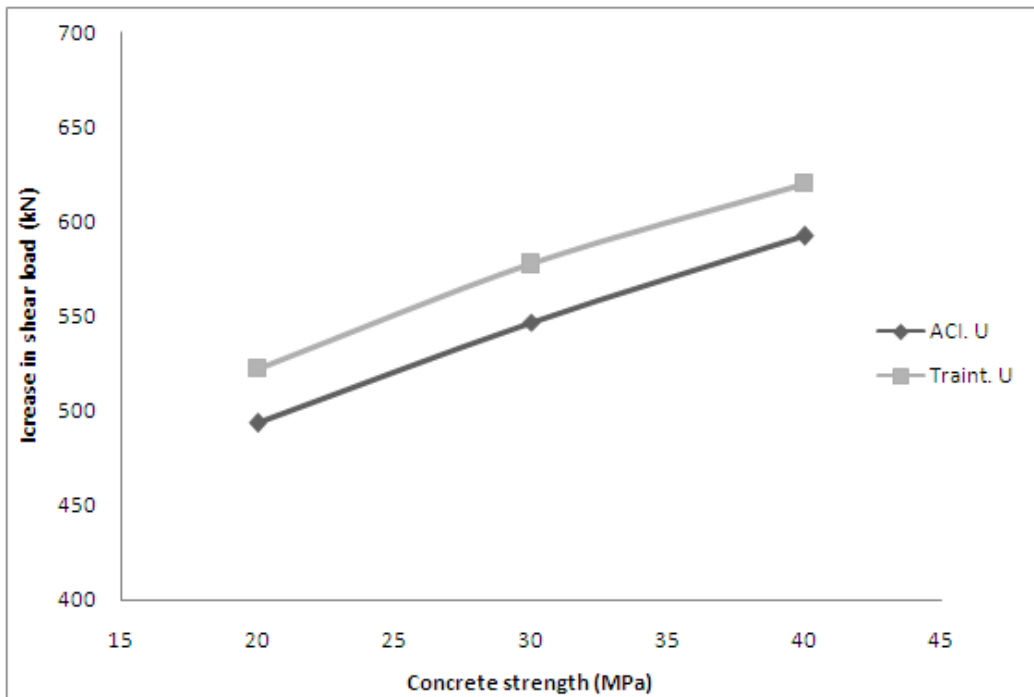
This study also includes the effect of compressive strength on shear capacity for different FRP configurations as shows in **Table 4.2** and **Fig.4.2**.

Table 4.2. The influence of concrete strength on concrete shear strength.

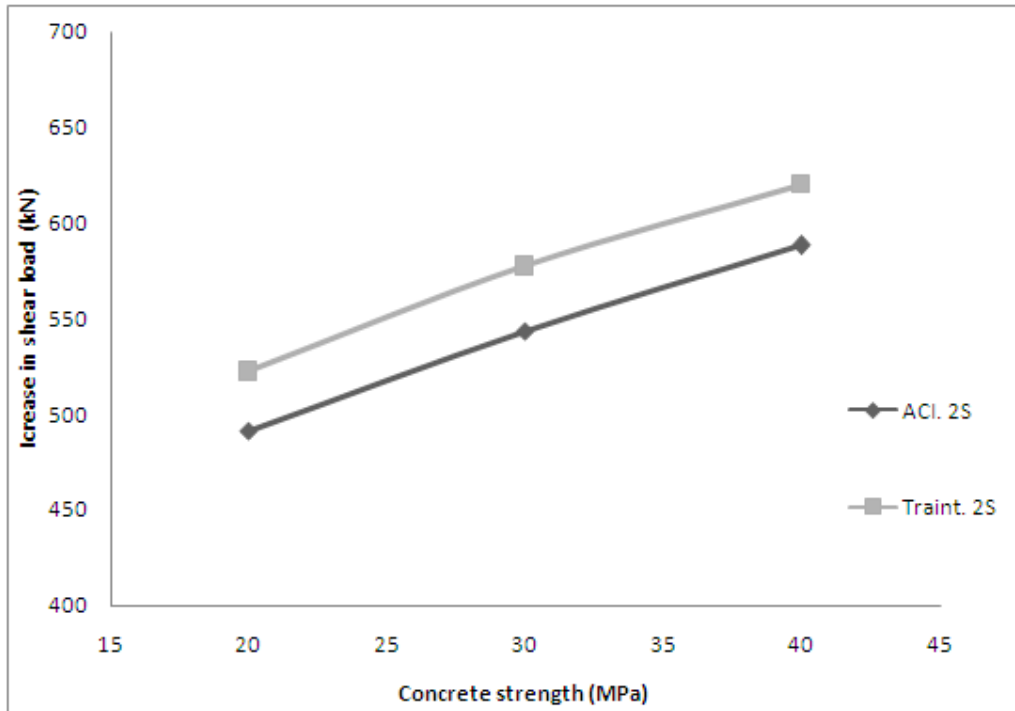
configurati on	compressive strength	ACI (kN)	Triant- afillou (kN)	Carolin (kN)	Zhichao (kN)	Percentage Of different		
						Triant- afillou	Carolin	Zhichao
Full warping	40MPa	699.6	541.2	562.2	549.6	22.6%	19.6%	21.4%
	30MPa	667.2	507.4	529.8	511.5	22.4%	20.6%	23.3%
	20MPa	628.8	467.2	491.4	466.7	25.7%	21.8%	25.8%
U- shape	40MPa	591.9	620.1	-	-	-4.8%		
	30MPa	546.5	577.3	-	-	-5.6%		
	20MPa	493.4	522.2	-	-	-5.8%		
Two side	40MPa	588.1	620.1	-	-	-5.4%		
	30MPa	543.3	577.3	-	-	-6.2%		
	20MPa	491.0	522.2	-	-	-6.3%		



(a)



(b)



(c)

Fig.4.2.Effect of concrete strength on concrete shear strength for different guidelines (a) full wrap (b) U- wrap (c) two sides.

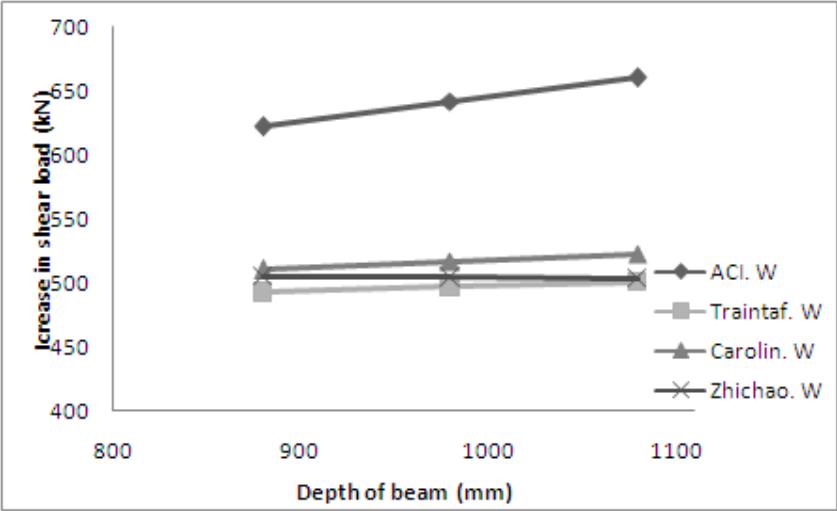
4.4. Effect of beam depth (d) on concrete shear strength (V_c)

This study also includes the effect of Beam Depth on shear capacity for different FRP configurations as shows in **Table 4.3** and **Fig. 4.3** , The Depth of FRP ,which consider was

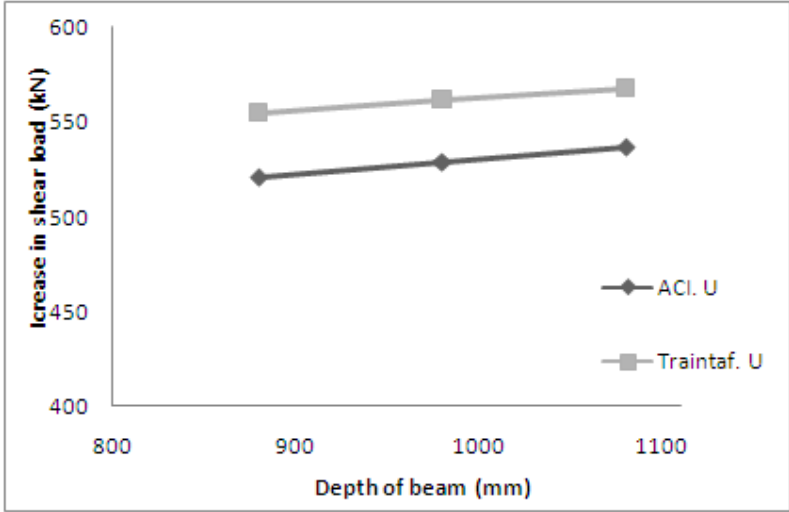
(1080mm), (980mm),(880mm) for different configuration.

Table 4.3. The influence of Beam Depth on shear Strength

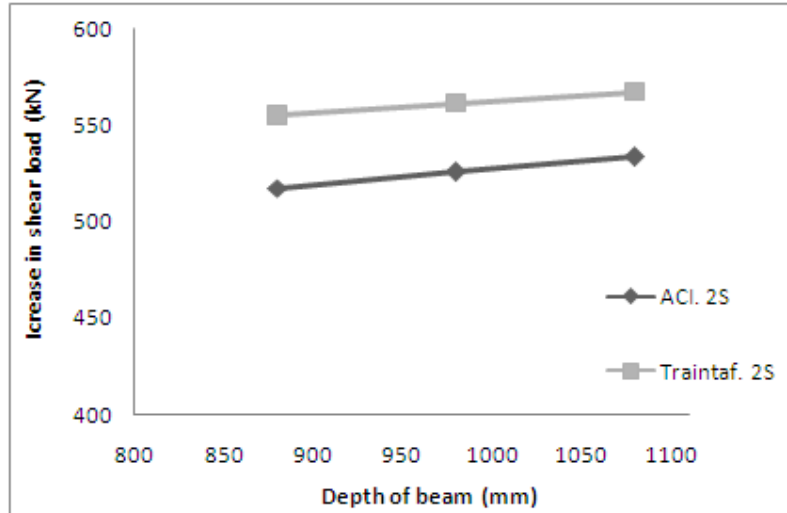
Config-uration	Beam Depth (mm)	ACI (Kn)	Triant-afillou (Kn)	Caroli n (Kn)	Zhichao (Kn)	Percentage Of Different		
						Triant-afillou	Carolin	Zhichao
Full warping	1080	660.18	500.0	522.7	503.2	24.2%	20.8%	23.7%
	980	641.2	496.4	516.5	503.8	23.5%	19.4%	21.4%
	880	621.8	492.4	509.9	504.5	20.8%	18%	18.8%
U- shape	1080	536.6	567.4	-	-	-5.7%		
	980	528.4	561.7	-	-	-6.3%		
	880	520.6	554.9	-	-	-6.5%		
Two side	1080	533.5	567.4	-	-	-6.3%		
	980	525.7	561.7	-	-	-6.8%		
	880	517.5	554.9	-	-	-7.2%		



(a)



(b)



(c)

Fig.4.3. Effect of beam depth on concrete shear strength (V_c) for different guidelines (a) full wrap (b) U wrap (c) two sides.

4.5. Discussion of results

In this study, it was considered effect of CFRP thickness on shear capacity as shown in **Table 4.1**. The following results were obtained:

1. For full wrap, it was appeared that ACI Method gave big values of shear capacity with respect to increase of CFRP thickness by Triantafillou, Carolin and Zhichao.
2. For U- and 2 sides wrapped, it was obvious that Triantafillou method gave significant values of shear capacity with respect to increase of thickness by ACI method.

The contribution of increasing the concrete compressive strength on shear capacity was also considered in this study as shown in **Table 4.2**. The results of shear capacity were summarized as follows:

1. For full wrapped it was found that ACI method gave significant values of shear capacity with respect to Triantafillou, Carolin and Zhichao.

2. For U- and 2 sides wrapped, it was appeared that Triantafillou gave the highest values of shear capacity with respect to ACI method.

Finally, it was also considered the effect of beams depth on shear capacity as shown in **Table 4.3**. The following results were obtained:

1. For full wrapped, it was found that ACI gave the highest values of shear capacity with respect to Triantafillou, Carolin and Zhichao.
2. For U-wrapped and 2 sides, Triantafillou gave the highest values of shear capacity with respect to ACI method.

CHAPTER FIVE

CONCLUSIONS AND RECOMMENDATIONS

CHAPTER FIVE

CONCLUSIONS AND RECOMMENDATIONS

5.1. Conclusions

Based on the results of different design guidelines on reinforced concrete deep beams strengthened with fiber reinforcement polymer (CFRP) and reported in literature the following conclusions and recommendations can be drawn:

- i. For CFRP shear contribution, the ACI equation is believed to be the most appropriate for practical design for the fully wrapped scheme. The ACI method appears to predict the (CFRP) shear contribution with a relatively high discrepancy with respect to Triantafillou, Carolin and Zhichao.
- ii. Presence of CFRP can increase the shear stiffness of deep beam. The ACI model predicted the ultimate capacity of deep beams base.
- iii. The use of ACI Method overestimates results of shear capacity for fully wrapped with respect to Triantafillou, Carolin and Zhichao.
- iv. The use of Triantafillou Method overestimates results of shear capacity for U, or two sides wrapped with respect to ACI Method.
- v. Carolin and Zhichao methods were used for full wrapped only.

5.2. Recommendations

Recommendation, were summarized as follows:

- i. The study of deep beam strengthening by CFRP need experimental work, but it was more expensive.
- ii. The modeling of CFRP reinforcement is needed using Computer Software.
- iii. Nonlinear analysis of deeps may be also done by computer software to predict the failure of deep beams.

REFERENCEC

1. Dischinger, F."Betrage Zur theories halbscheibe and des wandartigen balkns "publication I.A.B.S.E, Vol. I, 1932.
2. Mottock, A.H., Hawkins, N.M., "Research on shear transfer in reinforced concrete beams" PCI journal proceedings March, 1972.
3. De Pavia, H.A.R., Siess. C.p, "Strength and behavior of deep beams in shear", ASCE Journal proceedings, Oct 1965.
4. Besser, B., Macgregor, J.G "Review of concrete beams failing in shear", ASCE journal proceedings, Vol. 93, Feb 1967.
5. American Concrete Institute (ACI). (2008). "Guide for the design and construction of structural concrete reinforced with FRP bars." ACI 440.2R, Farmington Hills, MI.
6. M.A. Mansur, W.A.M. Alwis (1984) "Reinforced fibre concrete deep beams with web openings" international Journal of Cement Composites and Lightweight Concrete, Volume 6, Issue 4, November 1984, Pages 263-271.
7. Leonhardt, F. and Walther, R., wandartige trager Bulletin No.178, withern Ernst and Sohn Berlin, 1966,.
8. Kong, F.K., Robins, P.J, singh, A. and sharp, G.R,"Shearanalysis and design of reinforced concrete deep beams", The structural engineer, Vol.50, No.11, Oct. 1972,.
9. Prakash, D.,"A method for determing the shear strength of reinforced concrete beams with small a_v/d ratio". Magazine of concrete research, Vol. 79, no.3, march 1974.
10. Smith, K.N., and Vantsiots, A.S "deep beam test results compared with precast building code models " ACI Journal proceedings, Vol.79, No.3 July-Augest 1982.

11. Besser, I.I, and Cusens, A.R. "reinforced concrete deep beam panels with high depth/span ratios" Proc. Instu.Civil Eng.. Part2, June 1984.
12. Subidi, N.K., Alan, E.V., Kubota, N."reinforced concrete deep beams some tests results" magazine of concrete research, No.137, Dec 1986.
13. Kang, H.T., fung, K.K., Susanto, T., and Hai, y.L" main tension steel in high strength concrete deep and short beams". ACI Journal proceedings, No.6, Nov-Dec 1997.
14. Godat, A.,Qu, Z. Lu, Z.X.,Labossiere, P., Ye, P.L., Neale, WK & ASCE, M.(2010). "Size Effects for Reinforced Concrete Beams Strengthened in Shear with CFRP Strips". Journal of composites for construction, ASCE / MAY/JUNE 2010. pp. 260-271.
15. A.R. Khan¹, T. Ayub² (2009). "Performance of RC beams strengthened in shear by externally bonded u-shaped wraps". International Conference on Sustainable Built Environment Infrastructures in Developing Countries ENSET Oran (Algeria) - October 12-14, 2009.
16. Ahmed Sabry Farghaly and Brahim Benmokrane² (2013), "Shear Behavior of FRP-Reinforced Concrete Deep Beams without Web Reinforcement". ASCE, ISSN 1090-0268/04013015(10), April 13, 2013.
17. Shamsher B Singh, (2013)." Shear response and design of RC beams strengthened using CFRP laminates". International Journal of Advanced Structural Engineering 2013, 5:16.
18. Norazman Mohamad Nor, Mohd Hanif Ahmad Boestamam, and Mohammed Alias Yusof (2013), "Carbon Fiber Reinforced Polymer (CFRP) as Reinforcement for Concrete

- Beam”.International Journal of Emerging Technology and Advanced Engineering, Volume 3, Issue 2, February 2013).
19. Denise Ferreira; Eva Oller; Antonio Marí, M.ASCE; and Jesús Bairán (2013), “Numerical Analysis of Shear Critical RC Beams Strengthened in Shear with FRP Sheets”. J. Compos. Constr. 2013.17. ISSN 1090-0268/04013016(11).
 20. Florent Baby, Ph.D.; Pierre Marchand; and François Toutlemonde, (2013), “Shear Behavior of Ultrahigh Performance Fiber-Reinforced Concrete Beams. I: Experimental Investigation”. J. Struct. Eng. 2014.140. ASCE, ISSN 0733-9445/04013111(10).
 21. K.V. VENKATESHA, K. BALAJI Rao, S.V. DINESH (2012), “Experimental Investigation of Reinforced Concrete Beams With and Without CFRP Wrapping”. SLOVA K UNIVERSITY OF TECHNOLOG Y (Slovak Journal of Civil Engineering), Vol. XX, 2012, No. 3, 15 – 26.
 22. El Mostafa Higazy* and Mahmoud El-Kateb, (2011). “Strengthening of reinforced concrete beams under torsion using CFRP sheets”. Conference on our world in concrete & structures Singapore, august 14-16, 2011.
 23. G. M. Chen, J. G. Teng and J. F. Chen. (2010), “RC beams shear-strengthened with FRP”, Magazine of Concrete Research, 2010, 62, No. 4, April, 301–311.
 24. A. Godat; Z. Qu; X. Z. Lu; P. Labossière; L. P. Ye; and K. W. Neale, M.ASCE. (2010). (Size Effects for Reinforced Concrete Beams Strengthened in Shear with CFRP Strips”, Journal of Composites for Construction © ASCE / may/june 2010.
 25. Denvid Lau, Hoat Joen Pam. (2010). “Experimental study of hybrid FRP reinforced concrete beams”, Engineering structures -© 2010 Elsevier Ltd.

26. R. Balamuralikrishnan, and C. Antony Jeyasehar (2009), "Flexural Behavior of RC Beams Strengthened with Carbon Fiber Reinforced Polymer (CFRP) Fabrics". The Open Civil Engineering Journal, 2009, 3, 102-109.
27. Ma'en S. Abdel-Jaber, Anis S. Shatanawi and Mu'tasim S. Abdel-Jaber (2007). "Guidelines for Shear Strengthening of Beams Using Carbon Fibre-Reinforced Polymer (FRP) Plates". Jordan Journal of Civil Engineering, Volume 1, No. 4, 2007.
28. V.P.V. Ramana, T. Kant, S.E. Morton et al (2000), "Behavior of CFRPC strengthened reinforced concrete beams with varying degrees of strengthening". Elsevier Science Ltd- PII: S1359-8368(00)00022-6- Part B 31 (2000) 461-470.
29. Khalifa, A., Tumialan, G., Nanni, A. and Belarbi, A., "Shear Strengthening of Continuous RC Beams Using Externally Bonded CFRP Sheets," SP-188, American Concrete Institute, Proc., 4th International Symposium on FRP for Reinforcement of Concrete Structures (FRPRCS4), Baltimore, MD, Nov. 1999, pp. 995-1008.
30. Tom Norris, Hamid Saadatmanesh, Member, ASCE and Mohammad R. Ehsani (1997) "Shear and Flexural Strengthening of R/C Beams with Carbon Fiber Sheets". Journal of Structural Engineering, Vol. 123, No7, July 1997.
31. Chow, L., Conway, H.D, and Winter, G., s, stress in deep beams ASCE proceedings, May 1952.
32. Coull, A. "Stress analysis of deep beams and walls". The engineer, Vol,221 Feb 1966.
33. Prabhat, K. "Collapse load of deep reinforced concrete beams" Magaine of concrete research, No.94, March 1976.
34. Cheng, D.H and Pei, M.L "Continuous deep beams", ASCE Journal proceedings, structural division, No 45 June. 1954.

35. Ahmed M. Sayed; Xin Wang; and Zhishen Wu, M.ASCE. (2013).“Modelling of Shear Capacity of RC Beams Strengthened with CFRP Sheets Based on FE Simulation” J. Compos. Constr. 2013.17:687-701.
36. Meisam Safari Gorji (2009),” Analysis of FRP Strengthened Reinforced Concrete Beams Using Energy Variation Method”. World Applied Sciences Journal 6 (1): 105-111, 2009, ISSN 1818-4952.
37. Bengi Aykac, Ilker Kalkan, Sabahattin Aykac , Yusuf Emre Egriboz (2013) “Flexural behavior of RC beams with regular square or circular web Openings”, Engineering Structures 56 (2013) 2165–2174.
38. ACI 440-08, Guide for Design Construction of Externally Bonded FRP Systems for Strengthening Concrete Structures, July, 2008.

Appendix1: ACI code calculation sheet:(using ACI guide

1-Effect of FRP thickness t_f

a- For full warp

Effect of FRP thickness t_f			
Full Warp ($t_f=0.08$)			
no of strip (n) =	2	bw =	250 mm
FRP thich (t)	0.08	fc =	28 n/mm ²
Wf=	100 mm ²	df=	1080 mm
Afe =	32 mm ²	Ef=	223500
ffu =	3000	ε _{fu} =	0.018
Le = 23300/(n*t _f *E _f) ^{0.58} =	53.2581	sf=	200
k1= (fc/27) ^{2/3} =	1.02454		
k2= (df-Le)/df =	0.95069		for U warp
k2= (df-2Le)/df =	0.90137		for 2 sides warp
kv= (k1*k2*le)/11900 ε _{fu} ≤ 0.75 =			0.242177 OK
ε _{fe} = 0.004 ≤ 0.75*ε _{fu}	0.0135	0.004	for full warp
Vc= (fc) ^{0.5} *b*d	238117.618	Vs=	275300 N
Vf= (2wf*t _f *E _f *ε _{fe} *df)/sf=			260690.4 kN
Vs+Vf ≤ 0.66(fc) ^{0.5} *bw*d =			
Vn= VC+Vs+Vf =	0	+	774.108 ≤ 942.9458 kN
vn= .85VC+Vs+.70Vf =			660.1832553
P=			800

Full Warp (t=0.1)			
		bw =	250 mm
no of strip (n) =	2	fc =	28 n/mm2
FRP thich (t)	0.1	df=	1080 mm
Wf=	100 mm2	Ef=	223500
Afe =	40 mm2	ε _{fu} =	0.018
ffu =	3000	sf=	200
Le = 23300/(n*tf*Ef) ^{0.58} =	46.7926		
k1= (fc/27) ^{2/3} =	1.02454		
k2= (df-Le)/df =	0.95667		for U warp
k2= (df-2Le)/df =	0.91335		for 2 sides warp
kv= (k1*k2*le)/11900 ε _{fu} ≤ 0.75 =			
ε _{fe} =	0.004 ≤ 0.75*ε _{fu}	0.0135	0.004
			for full warp
ffe=	ε _{fe} *Ef =		894
Vc= (fc) ^{0.5} *b*d	238117.618	Vs=	275300 N
Vf= (2wf*tf*Ef*ε _{fe} *df)/sf=			325863 kN
Vs+Vf ≤ 0.66(fc) ^{0.5} *bw*d =			
Vn= Vc+Vs+Vf =	0	+	839.2806 ≤ 942.9458 kN
vn= .85Vc+Vs+.70Vf =			705.8040753

Full Warp (t=0.2)			
		bw =	250 mm
no of strip (n) =	2	fc =	28 n/mm2
FRP thich (t)	0.2	df=	1080 mm
Wf=	100 mm2	Ef=	223500
Afe =	80 mm2	ε _{fu} =	0.018
ffu =	3000	sf=	200
Le = 23300/(n*tf*Ef) ^{0.58} =	31.3026		
k1= (fc/27) ^{2/3} =	1.02454		
k2= (df-Le)/df =	0.97102		for U warp
k2= (df-2Le)/df =	0.94203		for 2 sides warp
kv= (k1*k2*le)/11900 ε _{fu} ≤ 0.75 =			
ε _{fe} =	0.004 ≤ 0.75*ε _{fu}	0.0135	0.004
			for full warp
ffe=	ε _{fe} *Ef =		3017.25
Vc= (fc) ^{0.5} *b*d	238117.618	Vs=	275300 N
Vf= (2wf*tf*Ef*ε _{fe} *df)/sf=			651726 N
Vs+Vf ≤ 0.66(fc) ^{0.5} *bw*d =			131195
Vn= Vc+Vs+Vf =	0	+	1165.144 ≤ 942.9458 kN
vn= .85Vc+Vs+.70Vf =			933.9081753

b-For U warp

U Warp (t=0.08)			
		bw =	250 mm
no of strip	2	fc =	28 n/mm ²
FRP thich	0.08	df=	1080 mm
Wf=	100 mm ²	Ef=	223500
Afe =	32 mm ²	ε _{fu} =	0.018
ffu =	3000	sf=	200
Le = 23300/(n*tf*Ef) ^{0.58} =	53.25806		
k1= (fc/27) ^{2/3} =	1.024541		
k2= (df-Le)/df =	0.950687		for U warp
k2= (df-2Le)/df =	0.901374		for 2 sides warp
kv= (k1*k2*le)/11900 ε _{fu} ≤ 0.75 =			0.242177 OK
ε _{fe} = kv*ε _{fu} ≤ 0.75 =		0.00435919	for U or 2 sides warp
ffe= ε _{fe} *Ef =		974.278207	
Vc= (fc) ^{0.5} *b*d/6=	238117.6		Vs= 275300 N
Vf= (2wf*tf*Ef*ε _{fe} *df)/sf=		84177.6371 N	
Vs+Vf ≤ 0.66(fc) ^{0.5} *bw*d =			
Vn= VC+Vs+Vf =	0	+ 597.595 ≤	942.9458 kN
vn= .85VC+Vs+.70Vf =		536.624321	
P=		800	

U Warp (t=0.1)			
		bw =	250 mm
no of strip	2	fc =	28 n/mm ²
FRP thich	0.1	df=	1080 mm
Wf=	100 mm ²	Ef=	223500
Afe =	40 mm ²	ε _{fu} =	0.018
ffu =	3000	sf=	200
Le = 23300/(n*tf*Ef) ^{0.58} =	46.79264		
k1= (fc/27) ^{2/3} =	1.024541		
k2= (df-Le)/df =	0.956673		for U warp
k2= (df-2Le)/df =	0.913347		for 2 sides warp
kv= (k1*k2*le)/11900 ε _{fu} ≤ 0.75 =			0.214117 OK
ε _{fe} = kv*ε _{fu} ≤ 0.75 =		0.00385411	for U or 2 sides warp
ffe= ε _{fe} *Ef =		861.393064	
Vc= (fc) ^{0.5} *b*d/6=	238117.6		Vs= 275300 N
Vf= (2wf*tf*Ef*ε _{fe} *df)/sf=		93030.4509 N	
Vs+Vf ≤ 0.66(fc) ^{0.5} *bw*d =			
VC+Vs+Vf=	0	+ 606.448 ≤	942.9458 kN
vn= .85VC+Vs+.70Vf =		542.821291	

U Warp (t=0.2)			
		bw =	250 mm
no of strip	2	fc =	28 n/mm ²
FRP thich	0.2	df=	1080 mm
Wf=	100 mm ²	Ef=	223500
Afe =	80 mm ²	ε _{fu} =	0.018
ffu =	3000	sf=	200
Le = 23300/(n*tf*Ef) ^{0.58} =	31.30258		
k1= (fc/27) ^{2/3} =	1.024541		
k2= (df-Le)/df =	0.971016		for U warp
k2= (df-2Le)/df =	0.942032		for 2 sides warp
kv= (k1*k2*le)/11900 ε _{fu} ≤ 0.75 =			0.145384 OK
ε _{fe} = kv*ε _{fu} ≤ 0.75 =		0.00261691	for U or 2 sides warp
ffe=	ε _{fe} *Ef =	584.879879	
Vc= (fc) ^{0.5} *b*d/6=	238117.6		
Vf= (2wf*tf*Ef*ε _{fe} *df)/sf=	126334.054 N	Vs=	275300 N
Vs+Vf ≤ 0.66(fc) ^{0.5} *bw*d =			
Vc+Vs+Vf=	639.752 ≤	942.9458 kN	
vn= .85Vc+Vs+.70Vf =	566.133813		

c-For two sides bond

side Warp (t=0.08)			
		bw =	250 mm
no of strip	2	fc =	28 n/mm ²
FRP thich	0.08	df=	1080 mm
Wf=	100 mm ²	Ef=	223500
Afe =	32 mm ²	ε _{fu} =	0.018
ffu =	3000	sf=	200
Le = 23300/(n*tf*Ef)	53.25806		
k1= (fc/27) ^{2/3} =	1.024541		
k2= (df-Le)/df =	0.950687		for U warp
k2= (df-2Le)/df =	0.901374		for 2 sides warp
kv= (k1*k2*le)/11900 ε _{fu} ≤ 0.75 =			0.229615 OK
ε _{fe} = kv*ε _{fu} ≤ 0.75 =		0.004133072	for U or 2 sides warp
ffe=	ε _{fe} *Ef =	923.7414871	
Vc= (fc) ^{0.5} *b*d/6=	238117.6		
Vf= (2wf*tf*Ef*ε _{fe} *df)/sf=	79811.26449 N	Vs=	275300 N
Vs+Vf ≤ 0.66(fc) ^{0.5} *bw*d =			
Vc+Vs+Vf=	593.2289 ≤	942.9458 kN	
vn= .85Vc+Vs+.70Vf =	533.5678604		
P=	800		

side Warp (t=0.1)			
		bw =	250 mm
no of strip	2	fc =	28 n/mm ²
FRP thich	0.1	df=	1080 mm
Wf=	100 mm ²	Ef=	223500
Afe =	40 mm ²	ε _{fu} =	0.018
ffu =	3000	sf=	200
Le = 23300/(n*tf*Ef)	46.79264		
k1= (fc/27) ² /3=	1.024541		
k2= (df-Le)/df =	0.956673		for U warp
k2= (df-2Le)/df =	0.913347		for 2 sides warp
kv= (k1*k2*le)/11900 ε _{fu} ≤ 0.75 =		0.20442 OK	
ε _{fe} = kv*ε _{fu} ≤ 0.75 =		0.00367956 for U or 2 sides warp	
ffe=	ε _{fe} *Ef =	822.3816728	
Vc= (fc) ^{0.5} *b*d/6=	238117.6		
Vf= (2wf*tf*Ef*ε _{fe} *df)/sf=	88817.22066 N	Vs=	275300 N
Vs+Vf ≤ 0.66(fc) ^{0.5} *bw*d =			
Vc+Vs+Vf=		602.2348 ≤	942.9458 kN
vn= .85Vc+Vs+.70Vf =		539.8720298	

side Warp (t=0.2)			
		bw =	250 mm
no of strip	2	fc =	28 n/mm ²
FRP thich	0.2	df=	1080 mm
Wf=	100 mm ²	Ef=	223500
Afe =	80 mm ²	ε _{fu} =	0.018
ffu =	3000	sf=	200
Le = 23300/(n*tf*Ef)	31.30258		
k1= (fc/27) ² /3=	1.024541		
k2= (df-Le)/df =	0.971016		for U warp
k2= (df-2Le)/df =	0.942032		for 2 sides warp
kv= (k1*k2*le)/11900 ε _{fu} ≤ 0.75 =		0.141044 OK	
ε _{fe} = kv*ε _{fu} ≤ 0.75 =		0.0025388 for U or 2 sides warp	
ffe=	ε _{fe} *Ef =	567.4217923	
Vc= (fc) ^{0.5} *b*d/6=	238117.6	Vs=	275300 N
Vf= (2wf*tf*Ef*ε _{fe} *df)/sf=	122563.1071 N		
Vs+Vf ≤ 0.66(fc) ^{0.5} *bw*d =			
Vc+Vs+Vf=		635.9807 ≤	942.9458 kN
vn= .85Vc+Vs+.70Vf =		563.4941503	

2- Effect of concrete

a- Full warp

Effect of concrete strength		for t=0.08				
Full Warp (fc=40)						
no of strip (n) =	2		bw =	250 mm		
FRP thich (t)	0.08		fc =	40 n/mm2		
Wf=	100 mm2		df=	1080 mm		
Afe =	32 mm2		Ef=	223500		
ffu =	3000		εfu =	0.018		
			sf=	200		
Le = 23300/(n*tf*Ef) ^{0.58} =		53.2581				
k1= (fc/27) ^{2/3} =		1.29956				
k2= (df-Le)/df =		0.95069			for U warp	
k2= (df-2Le)/df =		0.90137			for 2 sides warp	
kv= (k1*k2*le)/11900 εfu ≤ 0.75 =						
εfe =	0.004 ≤ 0.75*εfu	0.0135	0.004			for full warp
ffe=	εfe *Ef =		894			
Vc= (fc) ^{0.5} *b*d	284604.9894		Vs=	275300 N		
Vf= (2wf*tf*Ef*εfe*df)/sf=			260690.4 N			
Vs+Vf ≤ 0.66(fc) ^{0.5} *bw*d =						
Vc+Vs+Vf =			820.5954 ≤	1127.036 kN		
vn= .85Vc+Vs+.70Vf =			699.697521			

Full Warp (fc=30)						
no of strip (n) =	2		bw =	250 mm		
FRP thich (t)	0.08		fc =	30 n/mm2		
Wf=	100 mm2		df=	1080 mm		
Afe =	32 mm2		Ef=	223500		
ffu =	3000		εfu =	0.018		
			sf=	200		
Le = 23300/(n*tf*Ef) ^{0.58} =		53.2581				
k1= (fc/27) ^{2/3} =		1.07277				
k2= (df-Le)/df =		0.95069			for U warp	
k2= (df-2Le)/df =		0.90137			for 2 sides warp	
kv= (k1*k2*le)/11900 εfu ≤ 0.75 =						
εfe =	0.004 ≤ 0.75*εfu	0.0135	0.004			for full warp
ffe=	εfe *Ef =		894			
Vc= (fc) ^{0.5} *b*d	246475.1509		Vs=	275300 N		
Vf= (2wf*tf*Ef*εfe*df)/sf=			260690.4 N			
Vs+Vf ≤ 0.66(fc) ^{0.5} *bw*d =						
Vc+Vs+Vf =			782.4656 ≤	976.0416 kN		
vn= .85Vc+.70Vf =			667.2871582			

Full Warp (fc=20)			
		bw =	250 mm
no of strip (n) =	2	fc =	20 n/mm2
FRP thich (t)	0.08	df=	1080 mm
Wf=	100 mm2	Ef=	223500
Afe =	32 mm2	ε _{fu} =	0.018
ffu =	3000	sf=	200
Le = 23300/(n*tf*Ef) ^{0.58} =	53.2581		
k1= (fc/27) ^{2/3} =	0.81867		
k2= (df-Le)/df =	0.95069		for U warp
k2= (df-2Le)/df =	0.90137		for 2 sides warp
kv= (k1*k2*le)/11900 ε _{fu} ≤ 0.75 =			
ε _{fe} =	0.004 ≤ 0.75*ε _{fu}	0.0135	0.004
			for full warp
ffe=	ε _{fe} *Ef =	894	Vs= 275300 N
Vc= (fc) ^{0.5} *b*d	201246.118		
Vf= (2wf*tf*Ef*ε _{fe} *df)/sf=		260690.4 N	
Vs+Vf ≤ 0.66(fc) ^{0.5} *bw*d =			
Vc+Vs+Vf =		737.2365 ≤	796.9346 kN
vn= .85Vc+Vs+.70Vf =		628.8424803	

b-For U warp

U Warp (fc=40)			
		bw =	250 mm
no of strip	2	fc =	40 n/mm2
FRP thich	0.08	df=	1080 mm
Wf=	100 mm2	Ef=	223500
Afe =	32 mm2	ε _{fu} =	0.018
ffu =	3000	sf=	200
Le = 23300/(n*tf*Ef) ^{0.58} =	53.25806		
k1= (fc/27) ^{2/3} =	1.299563		
k2= (df-Le)/df =	0.950687		for U warp
k2= (df-2Le)/df =	0.901374		for 2 sides warp
kv= (k1*k2*le)/11900 ε _{fu} ≤ 0.75 =			0.307186 OK
ε _{fe} =	kv*ε _{fu} ≤ 0.75 =	0.00552934	for U or 2 sides warp
ffe=	ε _{fe} *Ef =	1235.80788	
Vc= (fc) ^{0.5} *b*d/6=	284605		
Vf= (2wf*tf*Ef*ε _{fe} *df)/sf=		106773.801 N	Vs= 275300 N
Vs+Vf ≤ 0.66(fc) ^{0.5} *bw*d =			
Vc+Vs+Vf=		666.679 ≤	1127.036 kN
vn= .85Vc+Vs+.70Vf =		591.955902	

U Warp (fc=30)					
			bw =	250 mm	
no of strip	2		fc =	30 n/mm ²	
FRP thich	0.08		df=	1080 mm	
Wf=	100 mm ²		Ef=	223500	
Afe =	32 mm ²		ε _{fu} =	0.018	
ffu =	3000		sf=	200	
Le = 23300/(n*tf*Ef) ^{0.58} =	53.25806				
k1= (fc/27) ^{2/3} =	1.072766				
k2= (df-Le)/df =	0.950687			for U warp	
k2= (df-2Le)/df =	0.901374			for 2 sides warp	
kv= (k1*k2*le)/11900 ε _{fu} ≤ 0.75 =				0.253576 OK	
ε _{fe} = kv*ε _{fu} ≤ 0.75 =			0.00456437		for U or 2 sides warp
ffe=	ε _{fe} *Ef =		1020.13693		
Vc= (fc) ^{0.5} *b*d/6=	246475.2			VS=	275300 N
Vf= (2wf*tf*Ef*ε _{fe} *df)/sf=			88139.8309 N		
Vs+Vf ≤ 0.66(fc) ^{0.5} *bw*d =					
Vc+Vs+Vf =			609.915 ≤	976.0416 kN	
vn= .85VC+Vs+.70Vf =			546.50176		

U Warp (fc=20)					
			bw =	250 mm	
no of strip	2		fc =	20 n/mm ²	
FRP thich	0.08		df=	1080 mm	
Wf=	100 mm ²		Ef=	223500	
Afe =	32 mm ²		ε _{fu} =	0.018	
ffu =	3000		sf=	200	
Le = 23300/(n*tf*Ef) ^{0.58} =	53.25806				
k1= (fc/27) ^{2/3} =	0.818674				
k2= (df-Le)/df =	0.950687			for U warp	
k2= (df-2Le)/df =	0.901374			for 2 sides warp	
kv= (k1*k2*le)/11900 ε _{fu} ≤ 0.75 =				0.193515 OK	
ε _{fe} = kv*ε _{fu} ≤ 0.75 =			0.00348327		for U or 2 sides warp
ffe=	ε _{fe} *Ef =		778.510184		
Vc= (fc) ^{0.5} *b*d/6=	201246.1				
Vf= (2wf*tf*Ef*ε _{fe} *df)/sf=			67263.2799 N	Vs=	275300 N
Vs+Vf ≤ 0.66(fc) ^{0.5} *bw*d =					
Vc+Vs+Vf =			543.809 ≤	796.9346 kN	
vn= .85VC+Vs+.70Vf =			493.443496		

c-For two sides bond

side Warp (fc=40)			
			bw = 250 mm
no of strip	2		fc = 40 n/mm ²
FRP thich	0.08		df= 1080 mm
Wf=	100 mm ²		Ef= 223500
Afe =	32 mm ²		ε _{fu} = 0.018
ffu =	3000		sf= 200
Le = 23300/(n*tf*Ef)	53.25806		
k1= (fc/27) ² /3=	1.299563		
k2= (df-Le)/df =	0.950687		for U warp
k2= (df-2Le)/df =	0.901374		for 2 sides warp
kv= (k1*k2*le)/11900 ε _{fu} ≤ 0.75 =			0.291252 OK
ε _{fe} = kv*ε _{fu} ≤ 0.75 =			0.00524253 for U or 2 sides warp
ffe=	ε _{fe} *Ef =		1171.705376
Vc= (fc) ^{0.5} *b*d/6=	284605		
Vf= (2wf*tf*Ef*ε _{fe} *df)/sf=	101235.3445 N	Vs=	275300 N
Vs+Vf ≤ 0.66(fc) ^{0.5} *bw*d =			
Vc+Vs+Vf =			661.1403 ≤ 1127.036 kN
vn= .85Vc+Vs+.70Vf =			588.0789821

side Warp (fc=30)			
			bw = 250 mm
no of strip	2		fc = 30 n/mm ²
FRP thich	0.08		df= 1080 mm
Wf=	100 mm ²		Ef= 223500
Afe =	32 mm ²		ε _{fu} = 0.018
ffu =	3000		sf= 200
Le = 23300/(n*tf*Ef)	53.25806		
k1= (fc/27) ² /3=	1.072766		
k2= (df-Le)/df =	0.950687		for U warp
k2= (df-2Le)/df =	0.901374		for 2 sides warp
kv= (k1*k2*le)/11900 ε _{fu} ≤ 0.75 =			0.240423 OK
ε _{fe} = kv*ε _{fu} ≤ 0.75 =			0.004327613 for U or 2 sides warp
ffe=	ε _{fe} *Ef =		967.221477
Vc= (fc) ^{0.5} *b*d/6=	246475.2		
Vf= (2wf*tf*Ef*ε _{fe} *df)/sf=	83567.93561 N	Vs=	275300 N
Vs+Vf ≤ 0.66(fc) ^{0.5} *bw*d =			
Vc+Vs+Vf =			605.3431 ≤ 976.0416 kN
vn= .85Vc+Vs+.70Vf =			543.3014332

side Warp (fc=20)			
		bw =	250 mm
no of strip	2	fc =	20 n/mm ²
FRP thich	0.08	df=	1080 mm
Wf=	100 mm ²	Ef=	223500
Afe =	32 mm ²	ε _{fu} =	0.018
ffu =	3000	sf=	200
Le = 23300/(n*tf*Ef)	53.25806		
k1= (fc/27) ² /3=	0.818674		
k2= (df-Le)/df =	0.950687		for U warp
k2= (df-2Le)/df =	0.901374		for 2 sides warp
kv= (k1*k2*le)/11900 ε _{fu} ≤ 0.75 =		0.183477 OK	
ε _{fe} = kv*ε _{fu} ≤ 0.75 =		0.003302587 for U or 2 sides warp	
ffe=	ε _{fe} *Ef =	738.1281336	
Vc= (fc) ^{0.5} *b*d/6=	201246.1		
Vf= (2wf*tf*Ef*ε _{fe} *df)/sf=	63774.27074 N	Vs=	275300 N
Vs+Vf ≤ 0.66(fc) ^{0.5} *bw*d =			
Vc+Vs+Vf =		540.3204 ≤	796.9346 kN
vn= .85Vc+Vs+.70Vf =		491.0011898	

2- Effect of beam depth d_f

a- Full warp

Full Warp (1080)			
		bw =	250 mm
no of strip (n) =	2	fc =	28 n/mm ²
FRP thich (t)	0.08	df=	1080 mm
Wf=	100 mm ²	Ef=	223500
Afe =	32 mm ²	ε _{fu} =	0.018
ffu =	3000	sf=	200
Le = 23300/(n*tf*Ef) ^{0.58} =	53.2581		
k1= (fc/27) ² /3=	1.02454		
k2= (df-Le)/df =	0.95069		for U warp
k2= (df-2Le)/df =	0.90137		for 2 sides warp
kv= (k1*k2*le)/11900 ε _{fu} ≤ 0.75 =			
ε _{fe} =	0.004 ≤ 0.75*ε _{fu}	0.0135	0.004 for full warp
ffe=	ε _{fe} *Ef =	894	
Vc= (fc) ^{0.5} *b*d	238117.618	Vs=	275300 N
Vf= (2wf*tf*Ef*ε _{fe} *df)/sf=	260690.4 N		
Vs+Vf ≤ 0.66(fc) ^{0.5} *bw*d =			
Vc+Vs+Vf =		774.108 ≤	942.9458 kN
vn= .85Vc+Vs+.70Vf =		660.1832553	

Full Warp (d=980)			
		bw =	272.72 mm
no of strip (n) =	2	fc =	28 n/mm ²
FRP thich (t)	0.08	df=	980.0293 mm
Wf=	100 mm ²	Ef=	223500
Afe =	32 mm ²	ϵ_{fu} =	0.018
ffu =	3000	sf=	200
Le = 23300/(n*tf*Ef) ^{0.58} =	53.2581		
k1= (fc/27) ^{2/3} =	1.02454		
k2= (df-Le)/df =	0.94566		for U warp
k2= (df-2Le)/df =	0.89131		for 2 sides warp
kv= (k1*k2*le)/11900 $\epsilon_{fu} \leq 0.75$ =			
ϵ_{fe} =	$0.004 \leq 0.75 * \epsilon_{fu}$	0.0135	0.004
			for full warp
ffe=	$\epsilon_{fe} * Ef$ =		894
Vc= (fc) ^{0.5} *b*d	235713.1592	Vs=	275300 N
Vf= (2wf*tf*Ef* ϵ_{fe} *df)/sf=		236559.4807 N	
Vs+Vf $\leq 0.66(fc)^{0.5} * bw * d$ =			
Vc+Vs+Vf =		747.5726 ≤	933.4241 kN
vn= .85Vc+Vs+.70Vf =		641.2478218	

Full Warp (d=880)			
		bw =	300 mm
no of strip (n) =	2	fc =	28 n/mm ²
FRP thich (t)	0.08	df=	880 mm
Wf=	100 mm ²	Ef=	223500
Afe =	32 mm ²	ϵ_{fu} =	0.018
ffu =	3000	sf=	200
Le = 23300/(n*tf*Ef) ^{0.58} =	53.2581		
k1= (fc/27) ^{2/3} =	1.02454		
k2= (df-Le)/df =	0.93948		for U warp
k2= (df-2Le)/df =	0.87896		for 2 sides warp
kv= (k1*k2*le)/11900 $\epsilon_{fu} \leq 0.75$ =			
ϵ_{fe} =	$0.004 \leq 0.75 * \epsilon_{fu}$	0.0135	0.004
			for full warp
ffe=	$\epsilon_{fe} * Ef$ =		894
Vc= (fc) ^{0.5} *b*d	232826.1154	Vs=	275300 N
Vf= (2wf*tf*Ef* ϵ_{fe} *df)/sf=		212414.4 N	
Vs+Vf $\leq 0.66(fc)^{0.5} * bw * d$ =			
Vc+Vs+Vf =		720.5405 ≤	921.9914 kN
vn= .85Vc+Vs+.70Vf =		621.8922781	

b-For U warp

U Warp (d=1080)			
		bw =	250 mm
no of strip	2	fc =	28 n/mm ²
FRP thich	0.08	df=	1080 mm
Wf=	100 mm ²	Ef=	223500
Afe =	32 mm ²	ε _{fu} =	0.018
ffu =	3000	sf=	200
Le = 23300/(n*tf*Ef) ^{0.58} =	53.25806		
k1= (fc/27) ^{2/3} =	1.024541		
k2= (df-Le)/df =	0.950687		for U warp
k2= (df-2Le)/df =	0.901374		for 2 sides warp
kv= (k1*k2*le)/11900 ε _{fu} ≤ 0.75 =			0.242177 OK
ε _{fe} = kv*ε _{fu} ≤ 0.75 =	0.00435919		for U or 2 sides warp
ffe= ε _{fe} *Ef =	974.278207		
Vc= (fc) ^{0.5} *b*d/6=	238117.6		
Vf= (2wf*tf*Ef*ε _{fe} *df)/sf=	84177.6371 N	Vs=	275300 N
Vs+Vf ≤ 0.66(fc) ^{0.5} *bw*d =			
Vc+Vs+Vf=	597.595 ≤		942.9458 kN
vn= .85Vc+Vs+.70Vf =	536.624321		

U Warp (d=980)			
		bw =	272.72 mm
no of strip	2	fc =	28 n/mm ²
FRP thich	0.08	df=	980.0293 mm
Wf=	100 mm ²	Ef=	223500
Afe =	32 mm ²	ε _{fu} =	0.018
ffu =	3000	sf=	200
Le = 23300/(n*tf*Ef) ^{0.58} =	53.25806		
k1= (fc/27) ^{2/3} =	1.024541		
k2= (df-Le)/df =	0.945657		for U warp
k2= (df-2Le)/df =	0.891313		for 2 sides warp
kv= (k1*k2*le)/11900 ε _{fu} ≤ 0.75 =			0.240896 OK
ε _{fe} = kv*ε _{fu} ≤ 0.75 =	0.00433612		for U or 2 sides warp
ffe= ε _{fe} *Ef =	969.123066		
Vc= (fc) ^{0.5} *b*d/6=	235713.2		
Vf= (2wf*tf*Ef*ε _{fe} *df)/sf=	75981.5227 N	Vs=	275300 N
Vs+Vf ≤ 0.66(fc) ^{0.5} *bw*d =			
Vc+Vs+Vf =	586.995 ≤		933.4241 kN
vn= .85Vc+Vs+.70Vf =	528.843251		

U Warp (d=880)			
		bw =	300 mm
no of strip	2	fc =	28 n/mm ²
FRP thich	0.08	df=	880 mm
Wf=	100 mm ²	Ef=	223500
Afe =	32 mm ²	ε _{fu} =	0.018
ffu =	3000	sf=	200
Le = 23300/(n*tf*Ef) ^{0.58} =	53.25806		
k1= (fc/27) ^{2/3} =	1.024541		
k2= (df-Le)/df =	0.939479		for U warp
k2= (df-2Le)/df =	0.878959		for 2 sides warp
kv= (k1*k2*le)/11900 ε _{fu} ≤ 0.75 =			0.239322 OK
ε _{fe} = kv*ε _{fu} ≤ 0.75 =	0.0043078		for U or 2 sides warp
ffe= ε _{fe} *Ef =	962.792589		
Vc= (fc) ^{0.5} *b*d/6=	232826.1		
Vf= (2wf*tf*Ef*ε _{fe} *df)/sf=	67780.5983 N	Vs=	275300 N
Vs+Vf ≤ 0.66(fc) ^{0.5} *bw*d =			
Vc+Vs+Vf =	575.907 ≤		921.9914 kN
vn= .85Vc+Vs+.70Vf =	520.648617		

c-For two sides bond

side Warp (d=1080)			
		bw =	250 mm
no of strip	2	fc =	28 n/mm ²
FRP thich	0.08	df=	1080 mm
Wf=	100 mm ²	Ef=	223500
Afe =	32 mm ²	ε _{fu} =	0.018
ffu =	3000	sf=	200
Le = 23300/(n*tf*Ef) ^{0.58} =	53.25806		
k1= (fc/27) ^{2/3} =	1.024541		
k2= (df-Le)/df =	0.950687		for U warp
k2= (df-2Le)/df =	0.901374		for 2 sides warp
kv= (k1*k2*le)/11900 ε _{fu} ≤ 0.75 =			0.229615 OK
ε _{fe} = kv*ε _{fu} ≤ 0.75 =	0.004133072		for U or 2 sides warp
ffe= ε _{fe} *Ef =	923.7414871		
Vc= (fc) ^{0.5} *b*d/6=	238117.6		
Vf= (2wf*tf*Ef*ε _{fe} *df)/sf=	79811.26449 N	Vs=	275300 N
Vs+Vf ≤ 0.66(fc) ^{0.5} *bw*d =			
Vc+Vs+Vf =	593.2289 ≤		942.9458 kN
vn= .85Vc+Vs+.70Vf =	533.5678604		

side Warp (d=980)			
		bw =	272.72 mm
no of strip	2	fc =	28 n/mm ²
FRP thich	0.08	df=	980.0293 mm
Wf=	100 mm ²	Ef=	223500
Afe =	32 mm ²	ε _{fu} =	0.018
ffu =	3000	sf=	200
Le = 23300/(n*tf*Ef)	53.25806		
k1= (fc/27) ² /3=	1.024541		
k2= (df-Le)/df =	0.945657		for U warp
k2= (df-2Le)/df =	0.891313		for 2 sides warp
kv= (k1*k2*le)/11900 ε _{fu} ≤ 0.75 =		0.227052 OK	
ε _{fe} = kv*ε _{fu} ≤ 0.75 =		0.004086941 for U or 2 sides warp	
ffe=	ε _{fe} *Ef =	913.4312048	
Vc= (fc) ^{0.5} *b*d/6=	235713.2		
Vf= (2wf*tf*Ef*ε _{fe} *df)/sf=	71615.15003 N	Vs=	275300 N
Vs+Vf ≤ 0.66(fc) ^{0.5} *bw*d =			
Vc+Vs+Vf =	582.6283 ≤		933.4241 kN
vn= .85Vc+Vs+.70Vf =	525.7867903		

side Warp (d=880)			
		bw =	300 mm
no of strip	2	fc =	28 n/mm ²
FRP thich	0.08	df=	880 mm
Wf=	100 mm ²	Ef=	223500
Afe =	32 mm ²	ε _{fu} =	0.018
ffu =	3000	sf=	200
Le = 23300/(n*tf*Ef)	53.25806		
k1= (fc/27) ² /3=	1.024541		
k2= (df-Le)/df =	0.939479		for U warp
k2= (df-2Le)/df =	0.878959		for 2 sides warp
kv= (k1*k2*le)/11900 ε _{fu} ≤ 0.75 =		0.223905 OK	
ε _{fe} = kv*ε _{fu} ≤ 0.75 =		0.004030292 for U or 2 sides warp	
ffe=	ε _{fe} *Ef =	900.7702507	
Vc= (fc) ^{0.5} *b*d/6=	232826.1		
Vf= (2wf*tf*Ef*ε _{fe} *df)/sf=	63414.22565 N	Vs=	275300 N
Vs+Vf ≤ 0.66(fc) ^{0.5} *bw*d =			
Vc+Vs+Vf =	571.5403 ≤		921.9914 kN
vn= .85Vc+Vs+.70Vf =	517.592156		

Appendix2: (Triantafillou and Anton 2000)

1-Effect of FRP thickness t_f

a- Full warp

Effect of FRP thickness t_f			
Full Warp (t=.08)			
a/d =	0.5	bw =	250 mm
no of strip	2	fc =	28 n/mm ²
FRP thich	0.08	df=	1080 mm
Wf=	100 mm ²	Ef=	223500
Afe =	32 mm ²	ϵ_{fu} =	0.018
ffu =	3000	sf=	200
pf =	$(2w_f*t_f)/b*s_f$	0.00032	
$\Gamma_f = (E_f * pf)/f_c^{2/3}(a/d) =$		15.51263	if (a/d) included
$\epsilon_{fe} =$	$0.72*\epsilon_{fu}*e^{-.0431*\Gamma_f} =$		for 2 or 3 side warp
$\epsilon_{fe} =$	$0.17(f_c^{2/3}/E_f*pf)^{0.3*\epsilon_{fu}} =$	0.001655	for full warp
$V_c = (f_c)^{0.5}*b*d/6 = 238117.6$			
$V_f = (2w_f*t_f*E_f*\epsilon_{fe}*df)/s_f =$	31960.68 N	$V_s =$	275300 N
$V_s + V_f \leq 0.66(f_c)^{0.5} * b*w*d =$			
$V_n = V_c + V_s + V_f =$	0 +	545.4	\leq 942.9458 kN
$v_n = .85V_c + V_s + .70V_f =$	500.0725		

Full Warp (t=0.1)			
a/d =	0.5	bw =	250 mm
no of strip	2	fc =	28 n/mm ²
FRP thich	0.1	df=	1080 mm
Wf=	100 mm ²	Ef=	223500
Afe =	40 mm ²	ϵ_{fu} =	0.018
ffu =	3000	sf=	200
pf =	$(2w_f*t_f)/b*s_f =$	0.0004	
$\Gamma_f = (E_f * pf)/f_c^{2/3}(a/d) =$		19.39079	if (a/d) included
$\epsilon_{fe} =$	$0.72*\epsilon_{fu}*e^{-.0431*\Gamma_f} =$	0.01295	for 2 or 3 side warp
$\epsilon_{fe} =$	$0.17(f_c^{2/3}/E_f*pf)^{0.3*\epsilon_{fu}} =$	0.001548	for full warp
$V_c = (f_c)^{0.5}*b*d/6 = 238117.6$			
$V_f = (2w_f*t_f*E_f*\epsilon_{fe}*df)/s_f =$	37363.97 N	$V_s =$	275300 N
$V_s + V_f \leq 0.66(f_c)^{0.5} * b*w*d =$			
$V_n = V_c + V_s + V_f =$		550.8	\leq 942.9458 kN
$v_n = .85V_c + V_s + .70V_f =$	503.8548		

Full Warp (t=0.2)			
a/d =	0.5	bw =	250 mm
no of strip	2	fc =	28 n/mm ²
FRP thich	0.2	df=	1080 mm
Wf=	100 mm ²	Ef=	223500
Afe =	80 mm ²	ε _{fu} =	0.018
ffu =	3000	sf=	200
pf =	(2wf*tf)/b*sf =	0.0008	
Γf = (Ef* pf)/fc ^{2/3} (a/d)=		38.78158	if (a/d) included
ε _{fe} =	0.72*ε _{fu} *e ^{-.0431*Γf} =	0.01295	for 2 or 3 side warp
ε _{fe} =	0.17(fc ^{2/3} /Ef*pf) ^{0.3*ε_{fu}} =	0.001257	for full warp
Vc= (fc) ^{0.5} *b*d/6= 238117.6			
Vf= (2wf*tf*Ef*ε _{fe} *df)/sf=	60697.95 N	Vs=	275300 N
Vs+Vf ≤ 0.66(fc) ^{0.5} *bw*d =			
Vn=Vc+Vs+Vf=	0 + 574.1 ≤	942.9458 kN	
vn= .85Vc+Vs+.70Vf =	520.1885		

b- U warp

U or 2 sides Warp (t=0.08)			
a/d =	0.5	bw =	250 mm
no of strip	2	fc =	28 n/mm ²
FRP thich	0.08	df=	1080 mm
Wf=	100 mm ²	Ef=	223500
Afe =	32 mm ²	ε _{fu} =	0.018
ffu =	3000	sf=	200
pf =	(2wf*tf)/b*sf =	0.00032	
e ^{-.0431*Γf} =	0.5124		
Γf = (Ef* pf)/fc ^{2/3} (a/d)=		15.51263166	if (a/d) included
ε _{fe} =	0.72*ε _{fu} *e ^{-.0431*Γf} =	0.006641	for 2 or 3 sides warp
ε _{fe} =	0.17(fc ^{2/3} /Ef*pf) ^{0.3*ε_{fu}} =	0.001655	for full warp
Vc= (fc) ^{0.5} *b*d/6= 238117.6			
Vf= (2wf*tf*Ef*ε _{fe} *df)/sf=	128234.6505 N	Vs=	275300 N
Vs+Vf ≤ 0.66(fc) ^{0.5} *bw*d =			
Vn=Vc+Vs+Vf=	641.652 ≤	942.9458 kN	
vn= .85Vc+Vs+.70Vf =	567.4642307		

U or 2 sides Warp (t=0.1)			
a/d =	0.5	bw =	250 mm
no of strip	2	fc =	28 n/mm ²
FRP thich	0.1	df=	1080 mm
Wf=	100 mm ²	Ef=	223500
Afe =	40 mm ²	ϵ_{fu} =	0.018
ffu =	3000	sf=	200
pf =	$(2wf*tf)/b*sf =$	0.0004	
$e^{-0.431*rf} =$	0.43355		
$\Gamma_f = (E_f * pf) / (f_c^{2/3} * a/d) =$	19.39078958	if (a/d) included	
$\epsilon_{fe} =$	$0.72 * \epsilon_{fu} * e^{-0.431 * \Gamma_f} =$	0.005619	for 2 or 3 sides warp
$\epsilon_{fe} =$	$0.17 * (f_c^{2/3} / E_f * pf)^{0.3 * \epsilon_{fu}} =$	0.001548	for full warp
Vc = (fc)^{0.5} * b * d / 6 = 238117.6			
Vf = (2wf*tf*Ef* ϵ_{fe} *df)/sf=	135626.7875 N	Vs=	275300 N
Vs+Vf ≤ 0.66(fc) ^{0.5} * bw * d =			
Vn=Vc+Vs+Vf=	649.044 ≤	942.9458 kN	
vn= .85Vc+Vs+.70Vf =	572.6387265		

U or 2 sides Warp (t=0.2)			
a/d =	0.5	bw =	250 mm
no of strip	2	fc =	28 n/mm ²
FRP thich	0.2	df=	1080 mm
Wf=	100 mm ²	Ef=	223500
Afe =	80 mm ²	ϵ_{fu} =	0.018
ffu =	3000	sf=	200
pf =	$(2wf*tf)/b*sf =$	0.0008	
$e^{-0.431*rf} =$	0.18796		
$\Gamma_f = (E_f * pf) / (f_c^{2/3} * a/d) =$	38.78157916	if (a/d) included	
$\epsilon_{fe} =$	$0.72 * \epsilon_{fu} * e^{-0.431 * \Gamma_f} =$	0.002436	for 2 or 3 sides warp
$\epsilon_{fe} =$	$0.17 * (f_c^{2/3} / E_f * pf)^{0.3 * \epsilon_{fu}} =$	0.001257	for full warp
Vc = (fc)^{0.5} * b * d / 6 = 238117.6			
Vf = (2wf*tf*Ef* ϵ_{fe} *df)/sf=	164637.8751 N	Vs=	275300 N
Vs+Vf ≤ 0.66(fc) ^{0.5} * bw * d =			
Vn=Vc+Vs+Vf=	678.055 ≤	942.9458 kN	
vn= .85Vc+Vs+.70Vf =	592.9464879		

2- Effect of concrete strength

a- Full warp

Full Warp fc=40)			
a/d =	0.5	bw =	250 mm
no of strip	2	fc =	40 n/mm2
FRP thich	0.08	df=	1080 mm
Wf=	100 mm2	Ef=	223500
Afe =	32 mm2	εfu =	0.018
ffu =	3000	sf=	200
pf =	(2wf*tf)/b*sf =	0.00032	
Γf = (Ef* pf)/fc ^{2/3} (a/d)=		12.22975	if (a/d) included
εfe =	0.72*εfu*e ^{-0.0431*Γf} =	0.01295	for 2 or 3 side warp
εfe =	0.17(fc ^{2/3} /Ef*pf) ^{0.3*εfu} =	0.001777	for full warp
Vc= (fc) ^{0.5} *b*d/6= 284605			
Vf= (2wf*tf*Ef*εfe*df)/sf=	34323.89 N	Vs=	275300 N
Vs+Vf ≤ 0.66(fc) ^{0.5} *bw*d =			
Vn=Vc+Vs+Vf=	0 + 594.2	≤	1127.036 kN
vn= .85Vc+Vs+.70Vf =	541.241		
Full Warp (fc=30)			
a/d =	0.5	bw =	250 mm
no of strip	2	fc =	30 n/mm2
FRP thich	0.08	df=	1080 mm
Wf=	100 mm2	Ef=	223500
Afe =	32 mm2	εfu =	0.018
ffu =	3000	sf=	200
pf =	(2wf*tf)/b*sf =	0.00032	
Γf = (Ef* pf)/fc ^{2/3} (a/d)=		14.81528	if (a/d) included
εfe =	0.72*εfu*e ^{-0.0431*Γf} =	0.01295	for 2 or 3 side warp
εfe =	0.17(fc ^{2/3} /Ef*pf) ^{0.3*εfu} =	0.001678	for full warp
Vc= (fc) ^{0.5} *b*d/6= 246475.2			
Vf= (2wf*tf*Ef*εfe*df)/sf=	32404.75 N	Vs=	275300 N
Vs+Vf ≤ 0.66(fc) ^{0.5} *bw*d =			
Vn=Vc+Vs+Vf=	0 + 554.2	≤	976.0416 kN
vn= .85Vc+Vs+.70Vf =	507.4872		

Full Warp (fc=20)			
a/d =	0.5	bw =	250 mm
no of strip	2	fc =	20 n/mm2
FRP thich	0.08	df=	1080 mm
Wf=	100 mm2	Ef=	223500
Afe =	32 mm2	εfu =	0.018
ffu =	3000	sf=	200
pf =	(2wf*tf)/b*sf =	0.00032	
Γf = (Ef* pf)/fc ^{2/3} (a/d)=		19.41351	if (a/d) included
εfe =	0.72*εfu*e ^{-0.431*Γf} =	0.01295	for 2 or 3 side warp
εfe =	0.17(fc ^{2/3} /Ef*pf) ^{0.3*εfu} =	0.001547	for full warp
Vc= (fc) ^{0.5} *b*d/6= 201246.1			
Vf= (2wf*tf*Ef*εfe*df)/sf=	29880.68 N	Vs=	275300 N
Vs+Vf ≤ 0.66(fc) ^{0.5} *bw*d =			
Vn=Vc+Vs+Vf=	506.4 ≤	796.9346 kN	
vn= .85VC+Vs+.70Vf =	467.2757		

b- U warp or two sides

U or 2 sides Warp (fc=40)			
a/d =	0.5	bw =	250 mm
no of strip	2	fc =	40 n/mm2
FRP thich	0.08	df=	1080 mm
Wf=	100 mm2	Ef=	223500
Afe =	32 mm2	εfu =	0.018
ffu =	3000	sf=	200
pf =	(2wf*tf)/b*sf =	0.00032	
e ^{-0.431*Γf} =	0.5875		
Γf = (Ef* pf)/fc ^{2/3} (a/d)=		12.22974797	if (a/d) included
εfe =	0.72*εfu*e ^{-0.431*Γf} =	0.007614	for 2 or 3 sides warp
εfe =	0.17(fc ^{2/3} /Ef*pf) ^{0.3*εfu} =	0.001777	for full warp
Vc= (fc) ^{0.5} *b*d/6= 284605			
Vf= (2wf*tf*Ef*εfe*df)/sf=	147029.3856 N	Vs=	275300 N
Vs+Vf ≤ 0.66(fc) ^{0.5} *bw*d =			
Vn=Vc+Vs+Vf=	706.934 ≤	1127.036 kN	
vn= .85VC+Vs+.70Vf =	620.1348109		

U or 2 sides Warp (fc=30)			
a/d =	0.5	bw =	250 mm
no of strip	2	fc =	30 n/mm2
FRP thich	0.08	df=	1080 mm
Wf=	100 mm2	Ef=	223500
Afe =	32 mm2	εfu =	0.018
ffu =	3000	sf=	200
pf =	(2wf*tf)/b*sf =	0.00032	
e ^{-0.431*rf} =	0.528		
Gf = (Ef* pf)/fc ^{2/3} (a/d)=	14.81528459	if (a/d) included	
ε _{fe} =	0.72*εfu*e ^{-0.431*rf} =	0.006843	for 2 or 3 sides warp
ε _{fe} =	0.17(fc ^{2/3} /Ef*pf) ^{0.3*εfu} =	0.001678	for full warp
Vc= (fc) ^{0.5} *b*d/6= 246475.2			
Vf= (2wf*tf*Ef*εfe*df)/sf=	132138.75 N	Vs=	275300 N
Vs+Vf ≤ 0.66(fc) ^{0.5} *bw*d =			
Vn=Vc+Vs+Vf=	0 +	653.914 ≤	976.0416 kN
vn= .85Vc+Vs+.70Vf =	577.3010032		

U or 2 sides Warp (fc=20)			
a/d =	0.5	bw =	250 mm
no of strip	2	fc =	20 n/mm2
FRP thich	0.08	df=	1080 mm
Wf=	100 mm2	Ef=	223500
Afe =	32 mm2	εfu =	0.018
ffu =	3000	sf=	200
pf =	(2wf*tf)/b*sf =	0.00032	
e ^{-0.431*rf} =	0.4331		
Gf = (Ef* pf)/fc ^{2/3} (a/d)=	19.41351479	if (a/d) included	
ε _{fe} =	0.72*εfu*e ^{-0.431*rf} =	0.005613	for 2 or 3 sides warp
ε _{fe} =	0.17(fc ^{2/3} /Ef*pf) ^{0.3*εfu} =	0.001547	for full warp
Vc= (fc) ^{0.5} *b*d/6= 201246.1			
Vf= (2wf*tf*Ef*εfe*df)/sf=	108388.8118 N	Vs=	275300 N
Vs+Vf ≤ 0.66(fc) ^{0.5} *bw*d =			
Vn=Vc+Vs+Vf=	0 +	584.935 ≤	796.9346 kN
vn= .85Vc+Vs+.70Vf =	522.2313685		

3- Effect of beam depth d_f

a- Full warp

Full Warp d=1080			
a/d =	0.5	bw =	250 mm
no of strip	2	fc =	28 n/mm ²
FRP thich	0.08	df=	1080 mm
Wf=	100 mm ²	Ef=	223500
Afe =	32 mm ²	ε _{fu} =	0.018
ffu =	3000	sf=	200
pf =	(2wf*tf)/b*sf =	0.00032	
Γf = (Ef* pf)/fc ^{2/3} (a/d)=		15.51263	if (a/d) included
ε _{fe} =	0.72*ε _{fu} *e ^{-0.0431*Γf} =	0.01295	for 2 or 3 side warp
ε _{fe} =	0.17(fc ^{2/3} /Ef*pf) ^{0.3} *ε _{fu} =	0.001655	for full warp
Vc= (fc) ^{0.5} *b*d/6= 238117.6			
Vf= (2wf*tf*Ef*ε _{fe} *df)/sf=	31960.68 kN	Vs=	275300 N
Vs+Vf ≤ 0.66(fc) ^{0.5} *bw*d =			
Vn=Vc+Vs+Vf=	0 + 545.4 ≤	942.9458 kN	
vn= .85Vc+Vs+.70Vf =	500.0725		

Full Warp (d=980)			
a/d =	0.5	bw =	272.72 mm
no of strip	2	fc =	28 n/mm ²
FRP thich	0.08	df=	980.0293 mm
Wf=	100 mm ²	Ef=	223500
Afe =	32 mm ²	ε _{fu} =	0.018
ffu =	3000	sf=	200
pf =	(2wf*tf)/b*sf =	0.000293	
Γf = (Ef* pf)/fc ^{2/3} (a/d)=		14.22029	if (a/d) included
ε _{fe} =	0.72*ε _{fu} *e ^{-0.0431*Γf} =	0.01295	for 2 or 3 side warp
ε _{fe} =	0.17(fc ^{2/3} /Ef*pf) ^{0.3} *ε _{fu} =	0.001699	for full warp
Vc= (fc) ^{0.5} *b*d/6= 235713.2			
Vf= (2wf*tf*Ef*ε _{fe} *df)/sf=	29769.01 kN	Vs=	275300 N
Vs+Vf ≤ 0.66(fc) ^{0.5} *bw*d =			
Vn=Vc+Vs+Vf=	0 + 540.8 ≤	933.4241 kN	
vn= .85Vc+Vs+.70Vf =	496.4945		

Full Warp (d=880)					
a/d =	0.5	bw =	300 mm	a =	1320
no of strip	2	fc =	28 n/mm ²		
FRP thich	0.08	df =	880 mm		
Wf =	100 mm ²	Ef =	223500		
Afe =	32 mm ²	ε _{fu} =	0.018		
ffu =	3000	sf =	200		
pf =	(2wf*tf)/b*sf =	0.000267			
e ^Λ .0431 =	0.957815				
Γf = (Ef* pf)/fc ^Λ / ₃ (a/d) =	12.92719			if (a/d) included	
ε _{fe} =	0.72*ε _{fu} *e ^Λ .0431*Γf =	0.01295			for 2 or 3 side warp
ε _{fe} =	0.17(fc ^Λ / ₃ /Ef*pf) ^Λ 0.3*ε _{fu} =	0.001748			for full warp
Vc = (fc) ^Λ 0.5*b*d/6 =	232826.1				
Vf = (2wf*tf*Ef*ε _{fe} *df)/sf =	27506.12 kN	Vs =	275300 N		
Vs+Vf ≤ 0.66(fc) ^Λ .5 *bw*d =					
Vn = Vc+Vs+Vf =	535.6	≤	921.9914 kN		
vn = .85Vc+Vs+.70Vf =	492.4565				

b-U warp or two sides

U or 2 sides Warp (d=1080)					
a/d =	0.5	bw =	250 mm		
no of strip	2	fc =	28 n/mm ²		
FRP thich	0.08	df =	1080 mm		
Wf =	100 mm ²	Ef =	223500		
Afe =	32 mm ²	ε _{fu} =	0.018		
ffu =	3000	sf =	200		
pf =	(2wf*tf)/b*sf =	0.00032			
e ^Λ 0.431*rf =	0.5124				
Γf = (Ef* pf)/fc ^Λ / ₃ (a/d) =	15.51263166			if (a/d) included	
ε _{fe} =	0.72*ε _{fu} *e ^Λ .0431*Γf =	0.006641			for 2 or 3 sides warp
ε _{fe} =	0.17(fc ^Λ / ₃ /Ef*pf) ^Λ 0.3*ε _{fu} =	0.001655			for full warp
Vc = (fc) ^Λ 0.5*b*d/6 =	238117.6				
Vf = (2wf*tf*Ef*ε _{fe} *df)/sf =	128234.6505 kN	Vs =	275300 N		
Vs+Vf ≤ 0.66(fc) ^Λ .5 *bw*d =					
Vn = Vc+Vs+Vf =	641.652	≤	942.9458 kN		
vn = .85Vc+Vs+.70Vf =	567.4642307				

U or 2 sides Warp (d=980)			
a/d =	0.5	bw =	272.72 mm
no of strip	2	fc =	28 n/mm2
FRP thich	0.08	df=	980.0293 mm
Wf=	100 mm2	Ef=	223500
Afe =	32 mm2	ϵ_{fu} =	0.018
ffu =	3000	sf=	200
pf =	$(2wf*tf)/b*sf =$	0.000293341	
$e^{-.0431*rf} =$	0.5417		
$\Gamma_f = (E_f * pf) / (f_c^{2/3} * (a/d)) =$	14.22029156	if (a/d) included	
$\epsilon_{fe} = 0.72 * \epsilon_{fu} * e^{-.0431 * \Gamma_f} =$	0.00702	for 2 or 3 sides warp	
$\epsilon_{fe} = 0.17 * (f_c^{2/3} / (E_f * pf))^{0.3} * \epsilon_{fu} =$	0.001699	for full warp	
Vc = (fc)^{0.5}*b*d/6= 235713.2			
Vf = (2wf*tf*Ef* ϵ_{fe} *df)/sf=	123018.4999 kN	Vs=	275300 N
Vs+Vf ≤ 0.66(fc) ^{0.5} *bw*d =			
Vn=Vc+Vs+Vf=	0 + 634.032	≤	933.4241 kN
vn = .85Vc+Vs+.70Vf =	561.7691352		

U or 2 sides Warp (d=880)			
a/d =	0.5	bw =	300 mm
no of strip	2	fc =	28 n/mm2
FRP thich	0.08	df=	880 mm
Wf=	100 mm2	Ef=	223500
Afe =	32 mm2	ϵ_{fu} =	0.018
ffu =	3000	sf=	200
pf =	$(2wf*tf)/b*sf =$	0.000266667	
$e^{-.0431*rf} =$	0.5729		
$\Gamma_f = (E_f * pf) / (f_c^{2/3} * (a/d)) =$	12.92719305	delete	if (a/d) included
$\epsilon_{fe} = 0.72 * \epsilon_{fu} * e^{-.0431 * \Gamma_f} =$	0.007425	for 2 or 3 sides warp	
$\epsilon_{fe} = 0.17 * (f_c^{2/3} / (E_f * pf))^{0.3} * \epsilon_{fu} =$	0.001748	for full warp	
Vc = (fc)^{0.5}*b*d/6= 232826.1			
Vf = (2wf*tf*Ef* ϵ_{fe} *df)/sf=	116824.5214 kN	Vs=	275300 N
Vs+Vf ≤ 0.66(fc) ^{0.5} *bw*d =			
Vn=Vc+Vs+Vf=	624.951	≤	921.9914 kN
vn = .85Vc+Vs+.70Vf =	554.979363		

Appendix3: carolin and Taljsten 2005

Full Warp (t= 0.08)					
a/d =	0.5	bw =	250 mm	β = (crack inlinatio	90
no of strip	2	fc =	28 n/mm2	α (frp direction)	45
FRP thich	0.08	df=	1080 mm	$\Theta = \alpha + \beta - 90 =$	45
Wf=	100 mm2	Ef=	223500	z =	1080
Afe =	32 mm2	$\epsilon_{fu} =$	0.018	$= \epsilon_{cr}$	
ffu =	3000	sf=	200		
n =	0.6	rf =bf/sf =	0.5		
pf =	$(2wf*tf)/b*sf =$		0.00032		
$\epsilon_{fe} = n \epsilon_{cr} =$			0.0108		
$\epsilon_{fe} =$					
Vc= (fc)^{0.5}*b*d/6= 238117.6					
$Vf = (n * \epsilon_{cr} * Ef * tf * rf * z * \cos\Theta) / \sin\alpha =$		64376.93 N	Vs=	275300 N	
$Vs + Vf \leq 0.66(fc)^{0.5} * bw * d =$					
$Vn = VC + Vs + Vf =$	0	+	577.8	\leq	942.9458 kN
$vn = .85VC + Vs + .70Vf =$			522.7638		

Full Warp (t= 0.1)					
a/d =	0.5	bw =	250 mm	β = (crack inlinatio	90
no of strip	2	fc =	28 n/mm2	α (frp direction)	45
FRP thich	0.1	df=	1080 mm	$\Theta = \alpha + \beta - 90 =$	45
Wf=	100 mm2	Ef=	223500	z =	1080
Afe =	40 mm2	$\epsilon_{fu} =$	0.018	$= \epsilon_{cr}$	
ffu =	3000	sf=	200		
n =	0.6	rf =bf/sf =	0.5		
pf =	$(2wf*tf)/b*sf =$		0.0004		
$\epsilon_{fe} = n \epsilon_{cr} =$			0.0108		
$\epsilon_{fe} =$					
Vc= (fc)^{0.5}*b*d/6= 238117.6					
$Vf = (n * \epsilon_{cr} * Ef * tf * rf * z * \cos\Theta) / \sin\alpha =$		80471.17 N	Vs=	275300 N	
$Vs + Vf \leq 0.66(fc)^{0.5} * bw * d =$					
$Vn = VC + Vs + Vf =$	0	+	593.9	\leq	942.9458 kN
$vn = .85VC + Vs + .70Vf =$			534.0298		

Full Warp (t= 0.2)					
a/d =	0.5	bw =	250 mm	β = (crack inlinatio	90
no of strip	2	fc =	28 n/mm2	α (frp direction)	45
FRP thich	0.2	df=	1080 mm	$\Theta = \alpha + \beta - 90 =$	45
Wf=	100 mm2	Ef=	223500	z =	1080
Afe =	80 mm2	$\epsilon_{fu} =$	0.018 = ϵ_{cr}		
ffu =	3000	sf=	200		
n =	0.6	rf =bf/sf =	0.5		
pf =	$(2wf*tf)/b*sf =$		0.0008		
$\epsilon_{fe} =$	$n \epsilon_{cr} =$		0.0108		
$\epsilon_{fe} =$					
Vc= (fc)^{0.5}*b*d/6= 238117.6					
Vf= (n *ϵ_{cr}*Ef*tf*rf*z*cosΘ)/sinα=		160942.3 N		Vs= 275300 N	
Vs+Vf\leq 0.66(fc)^{0.5}*bw*d =					
Vn= VC+Vs+Vf =		0 + 674.4 \leq		942.9458 kN	
vn= .85VC+Vs+.70Vf =		590.3596			

2- Effect of concrete strength

Full Warp (fc= 40)					
a/d =	0.5	bw =	250 mm	β = (crack inlinatio	90
no of strip	2	fc =	40 n/mm2	α (frp direction)	45
FRP thich	0.08	df=	1080 mm	$\Theta = \alpha + \beta - 90 =$	45
Wf=	100 mm2	Ef=	223500	z =	1080
Afe =	32 mm2	$\epsilon_{fu} =$	0.018 = ϵ_{cr}		
ffu =	3000	sf=	200		
n =	0.6	rf =bf/sf =	0.5		
pf =	$(2wf*tf)/b*sf =$		0.00032		
$\epsilon_{fe} =$	$n \epsilon_{cr} =$		0.0108		
$\epsilon_{fe} =$					
Vc= (fc)^{0.5}*b*d/6= 284605					
Vf= (n *ϵ_{cr}*Ef*tf*rf*z*cosΘ)/sinα=		64376.93 N		Vs= 275300 N	
Vs+Vf\leq 0.66(fc)^{0.5}*bw*d =					
Vn= VC+Vs+Vf =		0 + 624.3 \leq		1127.036 kN	
vn= .85VC+Vs+.70Vf =		562.2781			

Full Warp (fc= 30)					
a/d =	0.5	bw =	250 mm	β = (crack inlinatio	90
no of strip	2	fc =	30 n/mm2	α (frp direction)	45
FRP thich	0.08	df=	1080 mm	$\Theta = \alpha + \beta - 90 =$	45
Wf=	100 mm2	Ef=	223500	z =	1080
Afe =	32 mm2	$\epsilon_{fu} =$	0.018 = ϵ_{cr}		
ffu =	3000	sf=	200		
n =	0.6	rf =bf/sf =	0.5		
pf =	(2wf*tf)/b*sf =		0.00032		
$\epsilon_{fe} =$	n $\epsilon_{cr} =$		0.0108		
$\epsilon_{fe} =$					
Vc= (fc) ^{0.5} *b*d/6= 246475.2					
Vf= (n * ϵ_{cr} *Ef*tf*rf*z*cos Θ)/sin α =		64376.93 N	Vs=	275300 N	
Vs+Vf \leq 0.66(fc) ^{0.5} *bw*d =					
Vn= VC+Vs+Vf =		0 +	586.2 \leq	976.0416 kN	
vn= .85VC+Vs+.70Vf =			529.8677		

Full Warp (fc= 20)					
a/d =	0.5	bw =	250 mm	β = (crack inlinatio	90
no of strip	2	fc =	20 n/mm2	α (frp direction)	45
FRP thich	0.08	df=	1080 mm	$\Theta = \alpha + \beta - 90 =$	45
Wf=	100 mm2	Ef=	223500	z =	1080
Afe =	32 mm2	$\epsilon_{fu} =$	0.018 = ϵ_{cr}		
ffu =	3000	sf=	200		
n =	0.6	rf =bf/sf =	0.5		
pf =	(2wf*tf)/b*sf =		0.00032		
$\epsilon_{fe} =$	n $\epsilon_{cr} =$		0.0108		
$\epsilon_{fe} =$					
Vc= (fc) ^{0.5} *b*d/6= 201246.1					
Vf= (n * ϵ_{cr} *Ef*tf*rf*z*cos Θ)/sin α =		64376.93 N	Vs=	275300 N	
Vs+Vf \leq 0.66(fc) ^{0.5} *bw*d =					
Vn= VC+Vs+Vf =		0 +	540.9 \leq	796.9346 kN	
vn= .85VC+Vs+.70Vf =			491.4231		

3- Effect of beam depth (d)

Full Warp (d= 1080)					
a/d =	0.5	bw =	250 mm	β = (crack inlinatio	90
no of strip	2	fc =	28 n/mm2	α (frp direction)	45
FRP thich	0.08	df=	1080 mm	$\Theta = \alpha + \beta - 90 =$	45
Wf=	100 mm2	Ef=	223500	z =	1080
Afe =	32 mm2	$\epsilon_{fu} =$	0.018	$= \epsilon_{cr}$	
ffu =	3000	sf=	200		
n =	0.6	rf =bf/sf =	0.5		
pf =	$(2wf*tf)/b*sf =$		0.00032		
$\epsilon_{fe} =$	$n \epsilon_{cr} =$		0.0108		
$\epsilon_{fe} =$					
Vc= (fc)^{0.5}*b*d/6= 238117.6					
Vf= (n *ϵ_{cr}*Ef*tf*rf*z*cosΘ)/sinα=		64376.93 N		Vs= 275300 N	
Vs+Vf\leq 0.66(fc)^{0.5}*bw*d =					
Vn= VC+Vs+Vf =		0 + 577.8 \leq		942.9458 kN	
vn= .85VC+Vs+.70Vf =		522.7638			

Full Warp (d= 980)					
a/d =	0.5	bw =	272.72 mm	β = (crack inlinatio	90
no of strip	2	fc =	28 n/mm2	α (frp direction)	45
FRP thich	0.08	df=	980.0293 mm	$\Theta = \alpha + \beta - 90 =$	45
Wf=	100 mm2	Ef=	223500	z =	980.029
Afe =	32 mm2	$\epsilon_{fu} =$	0.018	$= \epsilon_{cr}$	
ffu =	3000	sf=	200		
n =	0.6	rf =bf/sf =	0.5		
pf =	$(2wf*tf)/b*sf =$		0.000293		
$\epsilon_{fe} =$	$n \epsilon_{cr} =$		0.0108		
$\epsilon_{fe} =$					
Vc= (fc)^{0.5}*b*d/6= 235713.2					
Vf= (n *ϵ_{cr}*Ef*tf*rf*z*cosΘ)/sinα=		58417.84 N		Vs= 275300 N	
Vs+Vf\leq 0.66(fc)^{0.5}*bw*d =					
Vn= VC+Vs+Vf =		0 + 569.4 \leq		933.4241 kN	
vn= .85VC+Vs+.70Vf =		516.5487			

Full Warp (d= 880)					
a/d =	0.5	bw =	300 mm	β = (crack inlinatio	90
no of strip	2	fc =	28 n/mm2	α (frp direction)	45
FRP thich	0.08	df=	880 mm	$\Theta = \alpha + \beta - 90 =$	45
Wf=	100 mm2	Ef=	223500	z =	880
Afe =	32 mm2	$\epsilon_{fu} =$	0.018	$= \epsilon_{cr}$	
ffu =	3000	sf=	200		
n =	0.6	rf =bf/sf =	0.5		
pf =	$(2wf*tf)/b*sf =$		0.000267		
$\epsilon_{fe} =$	$n \epsilon_{cr} =$	0.0108			
$\epsilon_{fe} =$					
Vc= (fc)^{0.5}*b*d/6= 232826.1					
Vf= (n *ϵ_{cr}*Ef*tf*rf*z*cosΘ)/sinα=		52455.28 N	Vs=	275300 N	
Vs+Vf\leq 0.66(fc)^{0.5}*bw*d =					
Vn= VC+Vs+Vf =		0 +	560.6	\leq	921.9914 kN
vn= .85VC+Vs+.70Vf =			509.9209		

Appendix4: Zhichao and cheng 2005

1-Effect of FRP thickness

For all Warp (t= 0.08)					
a/d =	0.5	bw =	250 mm		
no of strip	2	fc =	28 n/mm ²		
FRP thich	0.08	df=	1080 mm		
Wf=	100 mm ²	Ef=	223500		
Afe =	32 mm ²	ε _{fu} =	0.018		
ffu =	3000	sf=	200		
pf =	(2wf*tf)/b*sf =		0.00032		
R =	1.4871((pf*Ef/fc) ^{-.7488} =		0.736846103		
R =	0.5622(pf*Ef) ² - 1.2188(pf*Ef) + 0.778 =		0.693707	Or	
R =	(.0042(fc) ^{2/3} * wf)/(Ef*tf) ^{0.58} *ε _{fu} *df=		0.000681	which small	
ε _{fe} =	R* ε _{fu} =		2.04210454		
Vc= (fc) ^{0.5} *b*d/6=	238117.6				
Vf= (2wf*tf*Ef*ε _{fe} *df)/sf=		36512.82918 N	Vs=	275300 N	
Vs+Vf≤ 0.66(fc) ^{0.5} *bw*d =					
Vn=Vc+Vs+Vf=	0	+ 549.93 kN ≤	942.9458 kN		
vn= .85Vc+Vs+.70Vf =		503.2589557			

For all Warp (t= 0.1)					
a/d =	0.5	bw =	250 mm		
no of strip	2	fc =	28 n/mm ²		
FRP thich	0.1	df=	1080 mm		
Wf=	100 mm ²	Ef=	223500		
Afe =	40 mm ²	ε _{fu} =	0.018		
ffu =	3000	sf=	200		
pf =	(2wf*tf)/b*sf =		0.0004		
R =	0.5622(pf*Ef) ² - 1.2188(pf*Ef) + 0.778 =		0.673533	Or	
R =	(.0042(fc) ^{2/3} * wf)/(Ef*tf) ^{0.58} *ε _{fu} *df=		0.000598		
ε _{fe} =	R* ε _{fu} =		1.794197154		
Vc= (fc) ^{0.5} *b*d/6=	238117.6				
Vf= (2wf*tf*Ef*ε _{fe} *df)/sf=		40100.30638 N	Vs=	275300 N	
Vs+Vf≤ 0.66(fc) ^{0.5} *bw*d =					
Vn=Vc+Vs+Vf=	0	+ 553.518 kN ≤	942.9458 kN		
vn= .85Vc+Vs+.70Vf =		505.7701898			

For all Warp (t= 0.2)					
a/d =	0.5	bw =	250 mm		
no of strip	2	fc =	28 n/mm2		
FRP thich	0.2	df=	1080 mm		
Wf=	100 mm2	Ef=	223500		
Afe =	80 mm2	ε _{fu} =	0.018		
ffu =	3000	sf=	200		
pf =	(2wf*tf)/b*sf =		0.0008		
R =	0.5622(pf*Ef) ² - 1.2188(pf*Ef) + 0.778 =			0.578052	Or
R =	(.0042(fc) ² /3* wf)/(Ef*tf) ^{0.58} *ε _{fu} *df=			0.0004	
ε _{fe} =	R* ε _{fu} =		1.200252905		
Vc= (fc) ^{0.5} *b*d/6=	238117.6				
Vf= (2wf*tf*Ef*ε _{fe} *df)/sf=		53651.30486 N	Vs=	275300 N	
Vs+Vf≤ 0.66(fc) ^{0.5} *bw*d =					
Vn=Vc+Vs+Vf=	0	+	567.069 kN	≤	942.9458 kN
vn= .85Vc+Vs+.70Vf =			515.2558887		

2-Effect of concrete strength

for t=.08

For all Warp (fc= 40)					
a/d =	0.5	bw =	250 mm		
no of strip	2	fc =	40 n/mm2		
FRP thich	0.08	df=	1080 mm		
Wf=	100 mm2	Ef=	223500		
Afe =	32 mm2	ε _{fu} =	0.018		
ffu =	3000	sf=	200		
pf =	(2wf*tf)/b*sf =		0.00032		
R =	0.5622(pf*Ef) ² - 1.2188(pf*Ef) + 0.778 =			0.693707	Or
R =	(.0042(fc) ² /3* wf)/(Ef*tf) ^{0.58} *ε _{fu} *df=			0.000863	
ε _{fe} =	R* ε _{fu} =		2.590278499		
Vc= (fc) ^{0.5} *b*d/6=	284605				
Vf= (2wf*tf*Ef*ε _{fe} *df)/sf=		46314.17955 N	Vs=	275300 N	
Vs+Vf≤ 0.66(fc) ^{0.5} *bw*d =					
Vn=Vc+Vs+Vf=	0	+	606.219 kN	≤	1127.036 kN
vn= .85Vc+Vs+.70Vf =			549.6341667		

For all Warp (fc= 30)					
a/d =	0.5	bw =	250 mm		
no of strip	2	fc =	30 n/mm2		
FRP thich	0.08	df=	1080 mm		
Wf=	100 mm2	Ef=	223500		
Afe =	32 mm2	εfu =	0.018		
ffu =	3000	sf=	200		
pf =	(2wf*tf)/b*sf =	0.00032			
R =	0.5622(pf*Ef)^2 - 1.2188(pf*Ef) + 0.778 =			0.693707	Or
R =	(.0042(fc)^2/3* wf)/(Ef*tf)^0.58 *εfu*df=			0.000713	
εfe =	R* εfu=	2.138225739			
Vc= (fc)^0.5*b*d/6= 246475.2					
Vf= (2wf*tf*Ef*εfe*df)/sf=		38231.47621 N	Vs=	275300 N	
Vs+Vf≤ 0.66(fc)^.5 *bw*d =					
Vn=Vc+Vs+Vf=	0	+ 560.007 kN	≤	976.0416 kN	
vn= .85Vc+Vs+.70Vf =		511.5659116			

For all Warp (fc= 20)					
a/d =	0.5	bw =	250 mm		
no of strip	2	fc =	20 n/mm2		
FRP thich	0.08	df=	1080 mm		
Wf=	100 mm2	Ef=	223500		
Afe =	32 mm2	εfu =	0.018		
ffu =	3000	sf=	200		
pf =	(2wf*tf)/b*sf =	0.00032			
R =	0.5622(pf*Ef)^2 - 1.2188(pf*Ef) + 0.778 =			0.693707	Or
R =	(.0042(fc)^2/3* wf)/(Ef*tf)^0.58 *εfu*df=			0.000544	
εfe =	R* εfu=	1.631769433			
Vc= (fc)^0.5*b*d/6= 201246.1					
Vf= (2wf*tf*Ef*εfe*df)/sf=		29176.03745 N	Vs=	275300 N	
Vs+Vf≤ 0.66(fc)^.5 *bw*d =					
Vn=Vc+Vs+Vf=	0	+ 505.722 kN	≤	796.9346 kN	
vn= .85Vc+Vs+.70Vf =		466.7824265			

3-effect of beam depth(d)

for t=.08

For all Warp (d= 1080)					
a/d =	0.5	bw =	250 mm		
no of strip	2	fc =	28 n/mm2		
FRP thich	0.08	df=	1080 mm		
Wf=	100 mm2	Ef=	223500		
Afe =	32 mm2	ε _{fu} =	0.018		
ffu =	3000	sf=	200		
pf =	(2wf*tf)/b*sf =		0.00032		
R =	0.5622(pf*Ef) ² - 1.2188(pf*Ef) + 0.778 =			0.693707	Or
R =	(.0042(fc) ² /3* wf)/(Ef*tf) ^{0.58} *ε _{fu} *df=			0.000681	
ε _{fe} =	R* ε _{fu} =		2.04210454		
Vc= (fc) ^{0.5} *b*d/6= 238117.6					
Vf= (2wf*tf*Ef*ε _{fe} *df)/sf=		36512.82918 N	Vs=	275300 N	
Vs+Vf ≤ 0.66(fc) ^{0.5} *bw*d =					
Vn=Vc+Vs+Vf=	0	+	549.93 kN	≤	942.9458 kN
vn= .85Vc+Vs+.70Vf =			503.2589557		

For all Warp (d= 980)					
a/d =	0.5	bw =	272.72 mm		
no of strip	2	fc =	28 n/mm2		
FRP thich	0.08	df=	980.0293 mm		
Wf=	100 mm2	Ef=	223500		
Afe =	32 mm2	ε _{fu} =	0.018		
ffu =	3000	sf=	200		
pf =	(2wf*tf)/b*sf =		0.000293341		
R =	0.5622(pf*Ef) ² - 1.2188(pf*Ef) + 0.778 =			0.70051	Or
R =	(.0042(fc) ² /3* wf)/(Ef*tf) ^{0.58} *ε _{fu} *df=			0.00075	
ε _{fe} =	R* ε _{fu} =		2.250415193		
Vc= (fc) ^{0.5} *b*d/6= 235713.2					
Vf= (2wf*tf*Ef*ε _{fe} *df)/sf=		40237.42366 N	Vs=	275300 N	
Vs+Vf ≤ 0.66(fc) ^{0.5} *bw*d =					
Vn=Vc+Vs+Vf=	0	+	551.251 kN	≤	933.4241 kN
vn= .85Vc+Vs+.70Vf =			503.8223819		

For all Warp (d= 880)					
a/d =	0.5	bw =	300 mm		
no of strip	2	fc =	28 n/mm2		
FRP thich	0.08	df=	880 mm		
Wf=	100 mm2	Ef=	223500		
Afe =	32 mm2	ε _{fu} =	0.018		
ffu =	3000	sf=	200		
pf =	(2wf*tf)/b*sf =	0.000266667			
R =	0.5622(pf*Ef) ² - 1.2188(pf*Ef) + 0.778 =			0.707357	Or
R =	(.0042(fc) ² /3* wf)/(Ef*tf) ^{0.58} *ε _{fu} *df=			0.000835	
ε _{fe} =	R* ε _{fu} =	2.506219208			
V _c = (fc) ^{0.5} *b*d/6=	232826.1				
V _f = (2wf*tf*Ef*ε _{fe} *df)/sf=	44811.19945 N	V _s =	275300 N		
V _s +V _f ≤ 0.66(fc) ^{0.5} *bw*d =					
V _n =V _c +V _s +V _f =	0	+	552.937 kN	≤	921.9914 kN
v _n = .85V _c +V _s + .70V _f =			504.5700377		